## Dissolved Air Flotation (DAF) for Wastewater Treatment

Puganeshwary Palaniandy, Hj. Mohd Nordin Adlan, Hamidi Abdul Aziz, and Mohamad Fared Murshed

Universiti Sains Malaysia

Citation Information

Yung-Tse Hung

Waste Treatment in the Service and Utility Industries Edited by Yung - Tse Hung, Lawrence K . Wang, Mu - Hao Sung Wang, Nazih K . Shammas and Jiaping . Paul Chen Cleveland State University 6000 Broken Sound Parkway NW, Suite 300, Boca Raton, FL

33487-2742 CRC Press 2017 Print ISBN: 978-1-4200-7237-2

**CONTENTS** 

eBook ISBN: 978-1-351-67341-9

https://doi.org/10.1201/9781315164199

5.1	Introd	luction	146		
5.2	Types	s of Flotation	146		
	5.2.1	Electroflotation	146		
	5.2.2	Dispersed Air Flotation	147		
	5.2.3	Dissolved Air Flotation.			
5.3	Proce	ss Description of DAF	148		
5.4	Theory of DAF				
	5.4.1	Bubble Formation			
	5.4.2	Bubble-Particle Attachment	151		
	5.4.3	Flotation of Bubble–Particle Agglomerate	151		
	5.4.4	Kinetics of Flotation	151		
	5.4.5	Solubility of Air	157		
	5.4.6	Bubble Generation			
	5.4.7	Collision	160		
	5.4.8	Interception and Diffusion	163		
	5.4.9	Tank Design	166		
5.5	Advai	ntages of DAF Application in Wastewater Treatment	170		
5.6	Appli	cation of DAF Process in Wastewater Treatment	170		
5.7		cation of DAF Process in Landfill Leachate Treatment			
List	List of Nomenclature1				
Refe	rences		178		

#### Abstract

Flotation system consists of four major components—air supply, pressurizing pump, retention tank, and flotation chamber. The theory of dissolved air flotation (DAF) process is to separate suspended particles from liquids by bringing the particles to the surface of the liquid. In most cases, DAF is an alternative process to sedimentation and offers several advantages, including better final water quality, rapid startup, higher rates of operation, and thicker sludge. Additionally, DAF systems need less space compared with normal clarifiers, and due to their modular components, they allow easy installation and setup. This chapter covers types of flotation, process description of DAF, theory of DAF, advantages of DAF application in wastewater treatment, application of DAF process in wastewater treatment, and application of DAF in landfill leachate treatment.

## 5.1 INTRODUCTION

There are various types of flotation process available for different applications. The technology has been applied in many industries such as in mineral processing [1,2], wastewater clarification [3–6], artificial recharge [7], and potable water treatment [8,9]. Basically, flotation is a process of separating solids from a body of liquid by using air bubbles.

Flotation has been used in the mining and chemical processing industries for over 100 years [10]. However, the history of flotation goes back even earlier. The ancient Greeks used this process over 2000 years ago to separate minerals from gangue [11]. The development of the process to its current modern practices took several years. According to Kitchener, Haynes was able to separate minerals using oil in 1860 [12]. His method was patented. In 1905, Salman, Picard, and Ballot developed a process to separate sulfate grains from water by adding air bubbles and a small amount of oil to enhance the process. This was called "froth flotation." In 1910, T. Hoover developed the first flotation machine, which was not much different from the current equipment. A few years later, in 1914, Callow introduced a new process called "foam flotation" [12]. This process involved the introduction of air bubbles through submerged porous media. In fact, froth and foam flotation processes are generally known as dispersed air flotation processes and are used widely in the mineral processing industry. The development of the electrolytic flotation process can be traced back to 1904. The process was suggested by Elmore brothers who showed that electrolysis could produce bubbles for flotation. It was not used commercially at that time.

Dissolved air flotation was patented in 1924 by Niels Peterson and Carl Sveen in Scandinavia [13]. It was initially used to recover fibers and white water in the paper industry. The use of dissolved air flotation (DAF) in the treatment of wastewater and potable water began in the late 1960s. Edzwald and Walsh reported that DAF has been used for water clarification in Europe especially in the Scandinavian countries for more than 20 years, [10]. Heinanen, in his survey on the use of flotation in Finland, indicated that the first DAF plant for potable water clarification was constructed in 1965, and that by 1988, there were 34 plants in operation [14]. However the first application of flotation for a water reclamation plant was introduced in the early 1960s in South Africa [15]. In the United Kingdom, the first full-scale water treatment plant using this process was commissioned in 1976 at the Glendye Treatment Works of the Grampian Regional Council, Scotland [16]. Experiments carried out by researchers at the Water Research Centre showed that flotation is a more rapid method of solid–liquid separation than sedimentation [17].

## 5.2 TYPES OF FLOTATION

The basic idea in the flotation process is the solid–liquid separation process using bubbles. The bubbles are produced using any gas that is not highly soluble in liquid. However, in actual practice, air is the gas most commonly used because it is easily accessible, safe to use, and less expensive. The method of producing bubbles gives rise to different types of flotation processes, namely, electrolytic flotation, dispersed air flotation, and dissolved air flotation [18,19].

## 5.2.1 Electroflotation

Electrolytic flotation is also known as electroflotation. The bubbles are produced by passing a direct current between two electrodes and by generating oxygen and hydrogen in a diluted aqueous solution. Bubbles produced from electrolytic flotation are smaller compared with those produced from dispersed air flotation and DAF. Thus, this process is favorable for the removal of low-density fragile flocs. This process is suitable for effluent treatment [20], sludge thickening, and water treatment installations of  $10-20\,\mathrm{m}^3/\mathrm{h}$ . Figure 5.1 shows a typical arrangement of an electroflotation tank.

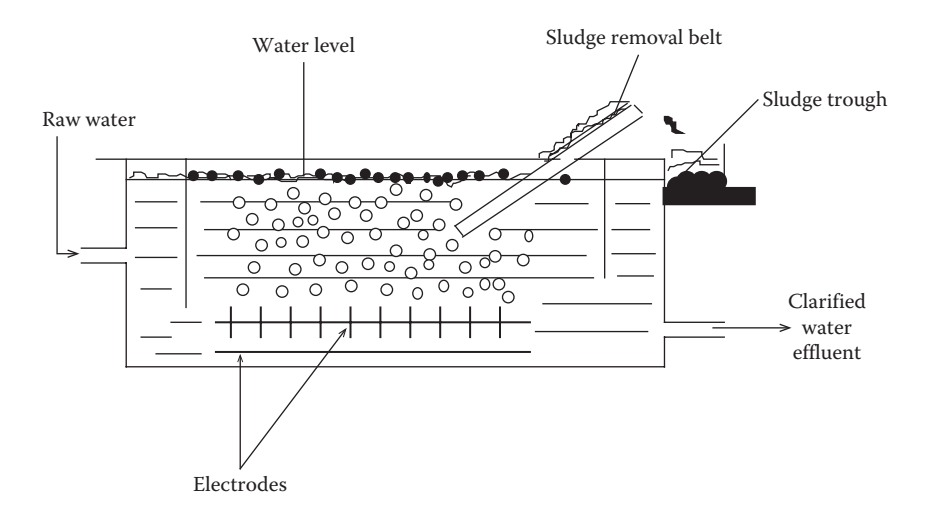


**FIGURE 5.1** Electroflotation tank. (From Adlan, M.N., A study of dissolved air flotation tank design variables and separation zone performance. PhD thesis, University of Newcastle Upon Tyne, 1998.)

#### 5.2.2 DISPERSED AIR FLOTATION

Dispersed air flotation has two different systems to generate bubbles, namely, foam flotation and froth flotation. In the foam flotation system, bubbles are generated by forcing air through a porous media made of ceramic, plastic, or sintered metal [21]. Figure 5.2 shows a typical arrangement for bubble generation through a medium or diffuser.

In the froth flotation system (shown in Figure 5.3), a high-speed impeller or turbine blade rotating in the solution is used to produce air bubbles.

Dispersed air flotation normally produces large air bubbles measuring >1 mm in diameter [22]. It is used mainly for the separation of minerals and removal of hydrophobic materials such as fat emulsions in selected wastewater treatment. This process was assessed for potable water treatment but was found unsuitable [23].

## 5.2.3 DISSOLVED AIR FLOTATION

The bubbles in DAF are produced by the reduction in pressure of a water stream saturated with air. The three types of DAF are vacuum flotation, microflotation, and pressure flotation, of which

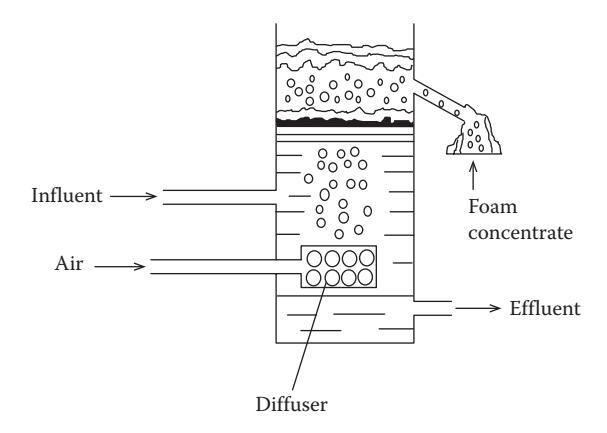


**FIGURE 5.2** Foam flotation. (From Adlan, M.N., A study of dissolved air flotation tank design variables and separation zone performance. PhD thesis, University of Newcastle Upon Tyne, 1998.)

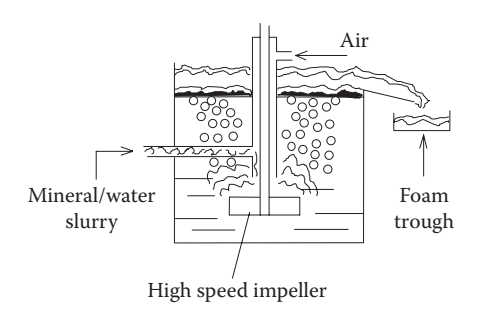


**FIGURE 5.3** Froth flotation. (From Adlan, M.N., A study of dissolved air flotation tank design variables and separation zone performance. PhD thesis, University of Newcastle Upon Tyne, 1998.)

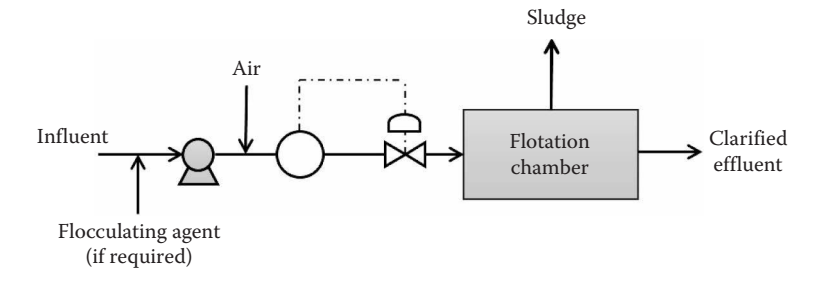


**FIGURE 5.4** Full flow pressure operational modes. (From Adlan, M.N., A study of dissolved air flotation tank design variables and separation zone performance. PhD thesis, University of Newcastle Upon Tyne, 1998.)

the pressure flotation is the most important and widely used in water and wastewater treatments. In the pressure flotation, the air is dissolved in water under high pressure and released at atmospheric pressure through a needle valve or nozzle, which produces small air bubbles.

There are three kinds of pressures dissolved in air flotation that can be used: full-flow, spilt-flow, and recycle flow pressure flotation [24,25].

- Full flow: The entire influent is pressurized and then released in the flotation tank, where
  the bubbles are formed. This type of flotation is used for influents that do not need flocculation but require large volumes of air bubbles (Figure 5.4).
- Spilt flow: A part of the influent is pressurized, and the remaining flows directly into the flocculation or flotation tank. This type of flow is cost-effective compared with full-flow pressure flotation, because the saturator and the feed pump handle only a portion of the total flow, thus requiring a smaller saturator and feed pump. However, split flow provides less air in the system. As a result, it has to be operated at high pressure to provide the same amount of air. This type of flow is used for influents containing suspended particles susceptible to the shearing effects of a pressure pump. It is also suitable for influents containing suspended particles at low concentration, due to low air requirement (Figure 5.5).
- Recycle flow: The influent flows into the flocculation or flotation tank if flocculation process is
  not required. A portion of the treated influent is recycled, pressurized, saturated with air, and
  released to the flotation tank. This type of flow is applied to influents that need coagulation and
  flocculation. It is a common type of flow, and it is used more often than other types (Figure 5.6).

#### 5.3 PROCESS DESCRIPTION OF DAF

The DAF system consists of air and water supply, saturator, and flotation chamber or tank. There are two types of flotation tanks: circular tank and rectangular tank. Wastewater treatment and sludge

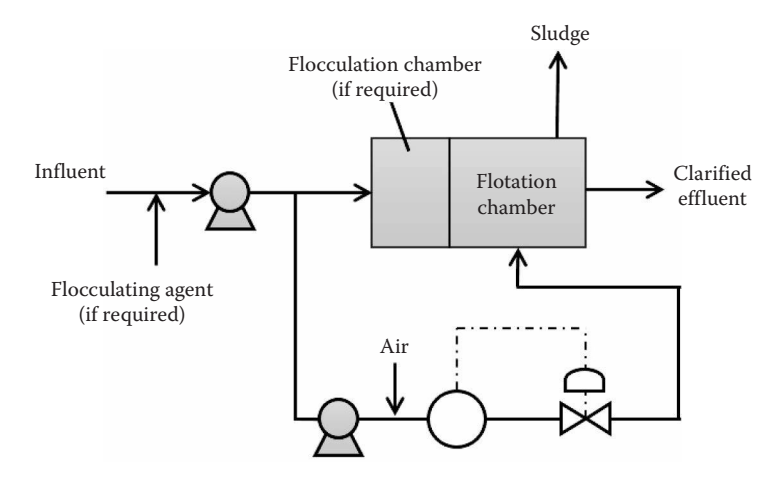


**FIGURE 5.5** Split flow operational modes. (From Adlan, M.N., A study of dissolved air flotation tank design variables and separation zone performance. PhD thesis, University of Newcastle Upon Tyne, 1998.)

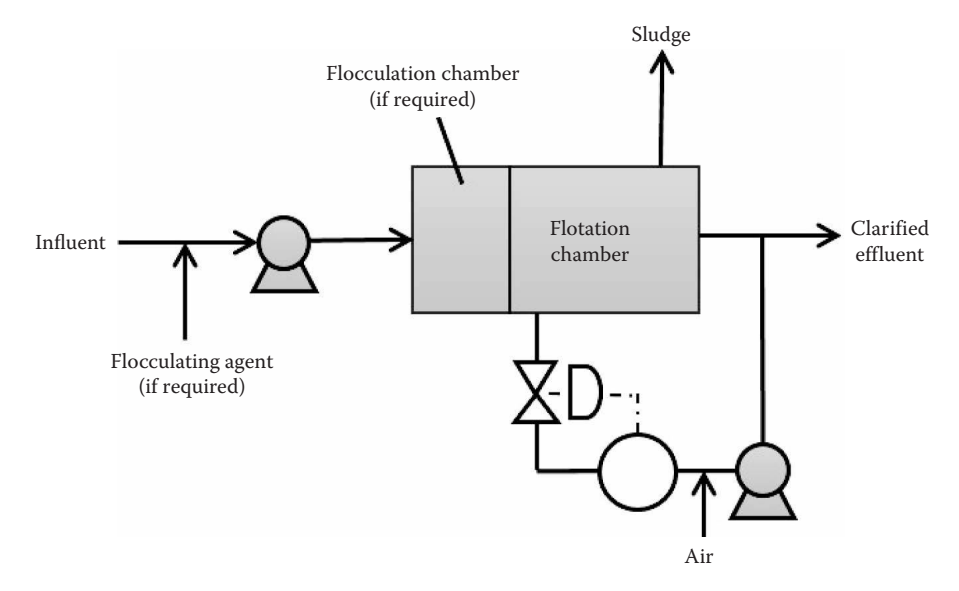


**FIGURE 5.6** Recycle flow operational mode. (From Adlan, M.N., A study of dissolved air flotation tank design variables and separation zone performance. PhD thesis, University of Newcastle Upon Tyne, 1998.)

thickening mostly use circular tanks in the flotation process, which is carried out in small-size flotation plants, and require no pre-flocculation prior to flotation. However, there are large flotation plants that use circular flotation tanks and include the flocculation process. Here, the flocculation and flotation processes are contained within the same circular tank to achieve an even distribution of bubbles and particles/flocs attachment. In contrast, the advantages of using rectangular flotation tanks are its simple design that makes the introduction of flocculated water into, and removal of the floated sludge from, the tank easier; simple dimensional scale-up; and the smaller area than the circular tank.

In rectangular tanks, an inclined baffle is fixed (60° to the horizontal or at 90°) between the contact zone and the separation zone. The baffle is fixed to elevate the bubble–floc agglomerates toward the surface. At the same time, the baffle also reduces the turbulence condition created by water/wastewater entering the separation zone. If the water/wastewater enters the separation zone at high velocity, it would create a turbulence condition, which would disturb the floated sludge layer

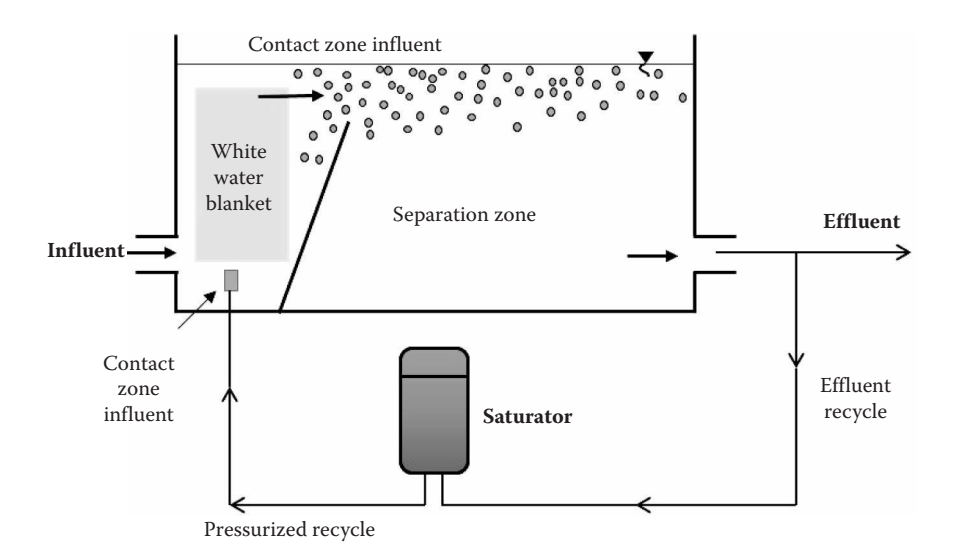


**FIGURE 5.7** Rectangular flotation tank with recycle flow system. (From Murshed, M.F., Removal of turbidity, suspended solid and aluminum using DAF pilot plant. MSc thesis, Universiti Sains Malaysia, 2007.)

that accumulates continuously on the surface of the flotation tank. Figure 5.7 shows a typical setup of a recycle flow DAF system with a rectangular flotation tank.

As can be seen in Figure 5.7, the flotation tank is divided into two zones: the front zone, which is the contact zone or reaction zone, and the separation zone. A baffle is fixed between the contact zone and the separation zone. The contact zone is designed to form bubble-floc agglomerates. Small air bubbles are introduced into the contact zone. To obtain the preferred bubble size, air is dissolved in a saturator under pressure in the range of 400-600 kPa. Thus, the pressure and the recycle flow control the total amount of air introduced into the contact zone [26]. Once the pressurized water is released into the flotation tank at atmospheric pressure, bubbles are produced. In DAF, small bubbles are required to achieve a good solid-liquid separation. Bubble size in the range of 50–100 µm is the most suitable for the DAF process. If the bubbles are larger than this range, they may create turbulence in the flotation tank and, at the same time, decrease the surface area of the bubble-particle attachment. Once the bubbles and particles come into contact through adhesion, trapping, or absorption process in the reaction zone, the bubble-floc aggregates move to the separation zone. Here, the bubble-floc aggregates will rise steadily to the surface of the flotation tank, while the treated water/wastewater will be withdrawn from the bottom of the tank. Later, the bubble-floc aggregates move to the separation zone. Here, the floc rises to the surface and floats as a thick layer of sludge. The rising velocity of the bubble-floc aggregates can be estimated using Stokes' law [27]. The aggregates that do not reach the surface are swept out with the clarified water.

## 5.4 THEORY OF DAF

To achieve a good solid–liquid separation using DAF for influents containing particles and natural color, coagulation or flocculation is necessary prior to the introduction of microbubbles to form bubble–floc aggregates [19]. The main idea in DAF is to float the particles having specific gravity more or less equal to the specific gravity of water. This should be carried out using a low-density gas bubble, usually air. The air bubbles adhere with the particles and reduce the specific gravity to <1.0, aggregate the particles, and float them to the surface of the flotation tank [28]. In DAF, there are three main processes for removal of particles: bubble formation, bubble–particle attachment, and flotation of the bubble–particle agglomerate [29].

## 5.4.1 Bubble Formation

There are two processes involved in bubble formation. First, the nucleation process, which initiates as soon as the pressurized water with air is released through the nozzle. The second step occurs when the excess air in the saturated water is transferred to the flotation tank in the form of gas. In this step, the bubbles begin to increase in size due to coalescence and decrease in hydrostatic pressure as they rise through the flotation tank. However, during this step, the air volume remains constant.

#### 5.4.2 Bubble-Particle Attachment

There are three types of bubble–particle attachment mechanisms:

- 1. Precipitation or collisions.
- 2. Bubbles trapped in a floc structure as the rise through the liquid medium.
- 3. Bubbles absorbed in a floc structure as the floc is formed.

The adhesion or collision, trapping, and absorption are sequence mechanisms in the bubble–particle attachment (Figure 5.8a through c). The particle must be destabilized to obtain good agglomeration between particle and bubble. However, the particle has to fulfil two most significant conditions: neutral charge and hydrophobic surface. Under these conditions, attachment between particle and bubble is very strong, resulting in successful flotation. Influent required coagulation process, a proper dosing and pH value resulting in low particle charge and the formation of hydrophobic particle surface.

#### 5.4.3 FLOTATION OF BUBBLE—PARTICLE AGGLOMERATE

In the DAF process, the particles float due to bubbles that reduce the density of the bubble–particle agglomerates. As long as bubble–particle agglomerates have lesser density than water (1.00 g/cm³), they will rise and float to the surface. If the particles are small, fewer bubbles are required to decrease the density compared with big particles that require more bubbles. The bubble–particle agglomerates should rise to the surface of the flotation tank [30]. The agglomerates that do not reach the surface are swept out with the clarified water. The rising velocity of the bubble–particle can be estimated using Stokes' law.

The three main theories in DAF show that there are some factors affecting the DAF system that should be taken into consideration before utilizing the DAF system in water or wastewater treatment. Therefore, the system operation and all factors should be accounted for in designing and utilizing the DAF system.

#### 5.4.4 KINETICS OF FLOTATION

Harper indicated that experiments seldom agree with the prediction that a bubble rising in a Newtonian liquid can be treated in isolation, unless great care is taken to remove impurities [31]. A bubble with constant surface tension rising under gravity will rise steadily if:

- 1. Its motion is stable relative to random small disturbances, and
- 2. The time taken to approach close to terminal velocity is much less than the time required for the bubble to change its size significantly.

At a low Reynolds number, the retarding or drag force is parallel and opposite to the terminal velocity with a magnitude of

$$D = 6\pi a\mu U, \tag{5.1}$$

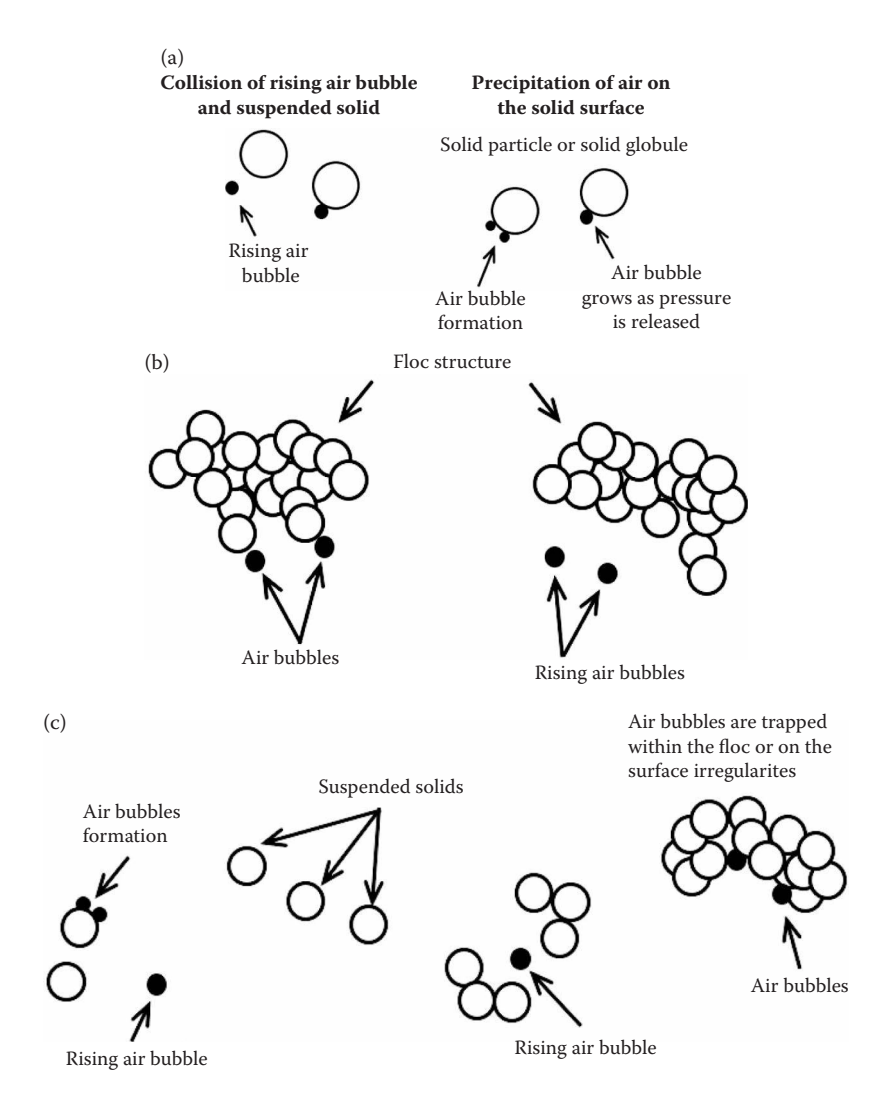


**FIGURE 5.8** Bubble–particle attachment mechanism (a)–(c). (a) Adhesion of air bubble, (b) rising air attaches to floc structure, and (c) entrapment within floc structure during formation. (From Adlan, M.N., A study of dissolved air flotation tank design variables and separation zone performance. PhD thesis, University of Newcastle Upon Tyne, 1998.)

#### where

D = drag force (kN) a = radius of bubble (m)  $\mu = \text{dynamic viscosity (kg/m/s)}$ U = terminal velocity (m/s)

Equation 5.1 was obtained by Stokes for slow motion of a sphere in viscous fluid [32,33]. The expression is usually known as Stokes' law for the resistance to a moving sphere [34]. The derivation of Stokes' law is based on the assumption that the motion of the spherical particle is extremely slow and that the liquid medium boundary is at an infinite distance from the particle and also is of a large volume compared with the dimensions of the particle [35]. Clift et al. showed that bubbles are closely approximated by spheres if the interfacial tension and/or viscous forces are much more important than inertia forces and the term "spherical" can be used if the ratio of minor axis to major axis lies within 10% of unity [36].

When a solid sphere falls vertically in a liquid, the viscous liquid produces a terminal velocity *U*. By equating the weight of the sphere to the sum of the up thrust and the drag [37], the following equation is obtained:

$$\frac{4}{3}\pi a^{3}\sigma g = \frac{4}{3}\pi a^{3}\rho g + 6\pi a\mu U$$

$$U = \frac{2}{9}(\sigma - \rho)a^{2}\frac{g}{\mu},$$
(5.2)

where

a = radius of sphere (m)  $\sigma = \text{density of sphere (kg/m}^3)$  $\rho = \text{density of liquid (kg/m}^3)$ 

Packham and Richards indicated that the alum sludge from a DAF water treatment plant rose at a rate of 20–35 mm/s [38]. The rising velocity is far greater than the settling velocity of an aluminum or iron floc encountered in a water treatment works (i.e., normally <0.5 mm/s). Basing their judgment on the fact that the rising rate of the floc in flotation was far greater than the settling rate, Packham and Richards considered the rate of separation of suspended matter in the flotation process from the viewpoint of Stokes' equation governing the motion of a sphere through a viscous medium and thus showed that Equation 5.2 was appropriate to describe the rising rate of the particle in the flotation process. Packham and Richards, in reviewing Equation 5.2, were of the opinion that if the size of the suspended matter is increased, a higher separation rate may be achieved. This is because the rate of separation is directly proportional to the square of the radius of the particles, the difference in the densities of liquid and the suspended particles, and inversely proportional to the liquid viscosity, as shown by Equation 5.2.

Research carried out in Russia [39] showed that at small Reynolds numbers, gas bubbles moved like solid spheres. Theoretical values of bubble rise velocity in water were not in agreement with much experimental data. For a gas bubble, which is assumed to behave like a solid, the surface can sustain a finite shear stress, the tangential velocity of the surface is everywhere zero relative to the center of the bubble, and the conventional Stokes' solution applies. According to Jameson, a force balance equation will result [40]:

$$6\pi\mu Ua = \frac{4}{3}\pi a^{3} (\rho - \rho_{g}) g. \tag{5.3}$$

When the density of gas  $\rho_g$  is negligible compared with the density of liquid  $\rho$ , the terminal velocity is given by

$$U = \frac{2\rho g a^2}{9\mu}. ag{5.4}$$

Equation 5.4 shows that the rise velocity of a bubble is controlled by the size of the bubble and the viscosity of the fluid. If the radius of the bubble is increased, the rise velocity will be increased. The kinematic viscosity is affected by the density and the temperature of the fluid. An increase in temperature will result in the decrease in viscosity, and hence an increase in rising velocity of the bubble. Shannon and Buisson indicated that bubble rise rates at  $80^{\circ}$ C increased three times compared with those at  $20^{\circ}$ C [41]. Force balance is presented in terms of drag coefficient  $C_D$  by Harper [31] as follows:

$$C_{\rm D} = \frac{\text{Force on bubble}}{1/2\rho U^2 \pi a^2} = \frac{4/3\pi \rho g a^3}{1/2\rho U^2 a^2} = \frac{4gd}{3U^2}.$$
 (5.5)

This coefficient is the force per unit cross-sectional area, made dimensionless by the dynamic pressure  $1/2\rho U^2$ . Substituting Equation 5.4 in 5.5 yields:

$$C_{\mathsf{D}} = \frac{24}{\mathsf{Re}},\tag{5.6}$$

where Re is the Reynolds number. Equation 5.6 is used for viscous resistance at low Reynolds numbers, Re < 0.5 [42]. The same equation was used by Vrablik to determine the maximum bubble size of  $130 \,\mu\text{m}$  for a complete viscous flow [43]. He indicated that the maximum value of the Reynolds number for laminar or viscous flow is 1.13. The relationship governing bubble size, laminar flow, bubble rising velocity (as per Equation 5.4), and temperature has been established. This relationship is shown in Table 5.1. The optimum bubble rising velocity for the DAF system is about 300 mm/min [44]. The rising velocity should not be  $<125 \, \text{mm/min}$  or  $>500 \, \text{mm/min}$ .

Experimental work by Fukushi et al. showed that Equation 5.4 cannot be used to describe bubble rise velocity [44]. This is due to the turbulent environment that occurs in the mixing zone (reaction zone) of the DAF tank. They suggested that the following equation is more appropriate and that it agreed with their experimental results:

$$U = \frac{pga^2}{3\mu}. (5.7)$$

The properties of air bubbles produced in the DAF process developed by Fukushi et al. were compared with those developed by Edzwald et al. [45,46]. There are many differences between the models. These are shown in Table 5.2. The model developed in 1985 by Fukushi et al. was based

TABLE 5.1
Relationship between Bubble Size, Rise Velocity, Temperature, and Laminar Flow

Bubble Size	Rise Velocity (m/h) Above Which Turbulent Flow Exists <sup>a</sup>		Terminal Rise Velocity (m/h) Based on Stokes' Law	
(μ <b>m</b> )	4°C	20°C	4°C	<b>20</b> °C
10	565	360	0.125	0.196
20	283	180	0.499	0.783
30	188	120	1.12	1.76
40	141	90	2.00	3.13
50	113	72	3.12	4.89
80	70.7	45	7.99	12.5
110	51.4	32.7	15.1	23.7
120	47.1	30	18.0	28.2
130	43.5	27.7	21.1	33.1 <sup>b</sup>
140	40.4	25.7	24.5	38.3b
160	35.3	22.5	31.9	50.1 <sup>b</sup>
170	33.2	21.2	36.1 <sup>b</sup>	56.5 <sup>b</sup>

Source: Malley, J.P. Jr., A fundamental study of dissolved air flotation for treatment of low turbidity waters containing natural organic matter. Unpublished Ph.D. dissertation, University of Massachusetts, 1988.

<sup>&</sup>lt;sup>a</sup> Based on a critical Reynold's number of 1.0 for the upper limit of laminar flow.

b Indicates that the terminal rise velocity will result in turbulent flow.

TABLE 5.2

Models Developed for the Dissolved Air Flotation Process

	Fukushi et al. [47]	Edzwald et al. [46]
	Generated Air Bubbles	
Size range $d_a$ (µm)	10–120 (average 60)	10-100 (average 40)
Rise velocity (cm/s)	$gd_a^2/12\nu$	$gd_{\rm a}^2/18\nu$
Zeta potential (mV)	−150 at pH 7	Not measured
Pressure P (kPa)	392	345–585
Recycle ratio r	0.1	0.08
Concentration $n_a$ (cm <sup>-3</sup> )	$10^4 - 10^5$	$10^4 - 10^5$
	<b>Produced Flocs</b>	
Size range $d_{\rm f}(\mu {\rm m})$	$10^0 - 10^3$	$10^{0}$ – $10^{2}$ (10–30 µm is best)
Density $\rho_f(g/cm^3)$	Floc density function	1.01 (assumed)
Suitable mobility (µm/s/V/cm)	0  to  + 1  (clay floc)	0.5 or less
	−1 to +1 (colour floc)	
	Bubble-Floc Collision and Attachment	
Collision model	Population balance model	Single collector collision model
Flow regime	Turbulent flow	Laminar flow
Mechanism	Locally isotropic turbulence, viscous subrange diffusion	Brownian diffusion, interception, gravity settling
Attachment mechanism	Electrical charge interactions (coverage of precipitated coagulant on a floc surface)	Electrical charge interaction, water layer at floc surface
Rise velocity of agglomerate (cm/s)	0.1–2.6 (observed)	About 0.3 (nearly equal to bubble rise velocity)

Source: Fukushi, K., et al., Water Sci. Technol., 31, 37-47, 1995.

g, gravity;  $d_a$ , diameter of bubble;  $\nu$ , kinematic viscosity;  $d_f$ , diameter of floc;  $\rho_f$ , density of floc.

on the population balance model of bubbles and flocs in a turbulent flow environment Population Balance Model (PBM model) [47]. However, the model developed by Edzwald was derived from a single collision theory in a laminar flow condition Single Collision Theory (SCT model). In the SCC model, collision occurs due to Brownian diffusion, interception, and gravity settling. Fukushi et al. indicated that Brownian diffusion and gravity settling cannot be dominant for a normal floc (10–1000 µm) and bubble size range in flotation [45]. Interception also cannot be dominant because, in practice, the mixing zone is apparently in a turbulent flow where certain energy dissipation occurs.

In fact, a literature survey indicates that Equation 5.7 was initially suggested by V. G. Levich in 1962. Levich showed that Equation 5.7 is applicable for small Reynolds numbers, *Re* << 1 and when the following inequality holds [48]:

$$\frac{ga^3}{3v^2} \ll 1,$$
 (5.8)

where  $v = \mu/\rho$  (i.e., kinematic viscosity equals dynamic viscosity divided by density of liquid). If the medium is water, the size of moving bubbles will be  $a << 2 \times 10^{-2}$  cm. Levich also indicated that the theoretical value of the drag coefficient for a gas bubble in water is equal to 8/Re (i.e., one and one-half times smaller than for a solid sphere). This value is not in agreement with Equation 5.6. However, Levich indicated that Allen's experimental results with small Reynolds

numbers completely disagreed with the theory and led to values for the drag coefficient that coincided exactly with the drag on a solid sphere [48].

A mathematical equation for solid/liquid separation was developed by Howe limited to flotation of discrete particles without the interference of surface-active forming agents. It was derived from a differential equation of motion, which was expanded to give solutions for the rising velocity of a particle with changes in the applied rising force, particle diameter, liquid viscosity, and particle density [49]. The equation is as follows:

$$R = 1 - e^{-\left(\frac{V_{\rm r}}{Q/A_{\rm h}}\right)},\tag{5.9}$$

where

R = ratio of total removal of solid concentration after flotation to the inflow solid concentration=  $1 - C_o/C_i$ 

 $C_{\rm o}$  = the effluent suspended solids

 $C_i$  = the influent suspended solids

 $V_r$  = the rising velocity of a single particle/air bubble (m/s)

Q = the flow applied to the flotation unit (m<sup>3</sup>/s)

 $A_{\rm h}$  = the horizontal area of the unit (m<sup>2</sup>)

Equation 5.9 is limited to discrete particles without the interference of surface-active forming agents. Karamanev, in his article on the rise of bubbles in quiescent liquid, showed that equations based on the model of bubble with internal circulation often fail to describe the real systems adequately [50]. This is because even highly purified liquids (such as triple distilled water) contain enough surface-active components to affect internal bubble recirculation. Recirculation is normally due to the presence of surface-active substances, and the resulting variable surface tension leads to a change in boundary conditions of the bubble [48]:

$$U = 25V^{1/6}, (5.10)$$

where V is the volume of the bubble. However, this equation works only for large, spherical capshaped bubbles. The drag coefficient  $C_D$  of the gas bubble calculated on the basis of equivalent sphere diameter by most authors was found to have a large deviation of  $C_D$  as a function of the Reynolds number when different liquids are used. The assumption made by most authors that free-falling heavy spheres behave exactly like free-rising solid spheres is found to be incorrect, especially for particles with densities <0.3 gm/cm<sup>3</sup> and Re>130 rising in water. Karamanev suggested the following equation based on the balance of forces acting on a rising bubble [50]:

$$\frac{1}{2}C_{\rm D}S\rho U^2 = \Delta\rho gV,\tag{5.11}$$

where  $\rho$  is the liquid density,  $\Delta \rho$  is the difference of density between liquid and gas, and S is the area of the bubble. To obtain  $C_D$  based on real bubble geometry, the area S should be determined from the diameter projected on the horizontal plane circle,  $d_h$ ;  $S = \pi d_h^2/4$ . Then, the volume of the bubble is calculated using the equivalent diameter,  $V = \pi d_e^3/6$ . These values are substituted in Equation 5.11 and become

$$C_{\rm D} = \frac{4g\Delta\rho d_{\rm e}^3}{3\rho d_{\rm h}^2 U^2}.$$
 (5.12)

Equation 5.11 can be written in terms of *U*:

$$U = \left(\frac{8gV}{\pi C_{\rm D} d_{\rm h}^2}\right)^{1/2}.$$
 (5.13)

By substituting from Equation 5.12,

$$U = \left(\frac{8g}{6^{2/3}\pi^{1/3}C_{\rm D}}\right)^{1/2}V^{1/6}\frac{d_{\rm e}}{d_{\rm h}}.$$
 (5.14)

For Re < 130, Karamanev suggested that  $C_D$  can be calculated using the following equation:

$$C_{\rm D} = \frac{24\left(1 + 0.173\,\mathrm{Re}^{0.657}\right)}{\mathrm{Re}} + \frac{0.413}{1 + 16300\,\mathrm{Re}^{-1.09}}.$$
 (5.15)

For spherical bubbles at Re < 1,  $C_D = 24/\text{Re}$  and  $d_e/d_h = 1 = 1$  and Equation 5.12 transforms to Stokes' equation.

## 5.4.5 SOLUBILITY OF AIR

In flotation, the quantities of air used are normally expressed in terms of volume of air supplied per volume of water treated [10]. Henry's law is used when treating saturated water as a dilute solution of air in water [43]. It must be remembered that Henry's law was originally based on his experiment with  $N_2$ ,  $O_2$ ,  $N_2O$ ,  $H_2S$ ,  $CO_2$  and water at only one temperature. The concept that the law could be used for general application is unfounded [51]. However, experimental work on wastewater with dissolved solids up to  $1000 \, \text{mg/L}$  with pressures up to  $500 \, \text{kPa}$  showed that Henry's law constant could be used to calculate the mass of dissolved air [52]. For ideal dilute solutions where the solute obeys Henry's law but not Raoult's law, and the solvent obeys Raoult's law, then the use of Henry's law is applicable [53,54].

$$PB = x_B K_B, (5.16)$$

where PB is the vapour pressure,  $x_B$  is the mole fraction of the solute, and  $K_B$  is constant. Based on Henry's law, Edzwald and Walsh suggested the following:

$$C_{\rm S} = f \frac{p}{k},\tag{5.17}$$

where  $C_S$  is the concentration of air in the saturated liquid, p is the absolute pressure, k is the Henry's law constant, and f is the efficiency factor, which is about 70% for unpacked saturators and up to 90% for packed systems. Values of k at 0°C and 25°C are 2.72 and 4.53 kPa/mg/L, respectively. However, others indicated that Henry's law is not strictly applicable when treating saturated water [55,56]. The equation has to be modified with an exponent m on the pressure p as follows [56]:

$$C_{\rm S} = \frac{p^{\rm m}}{k}.\tag{5.18}$$

Klassen and Mokrousov, in their review on the solubility of gases in water, were of the opinion that the solubility of gases depends on the partial pressure, temperature, and concentration of other substances in the solution [57]. If the partial pressure is increased, then the solubility of gas will be

increased. However, if the concentration of soluble substances in water is increased, gas solubility will be decreased as definite quantities of water molecules complex in the form of hydrated ions. Edwards added that if the total pressure is <507 kPa (5 atm.), the solubility for a particular partial pressure of solute gas is normally independent of the total pressure of the system [58]. In its relationship to temperature, the solubility of a gas will be decreased when the temperature is increased [43,59]. This is as illustrated in Figure 5.9. In the case of distilled water, when the temperature is increased from 0°C to 30°C, the solubility of air is reduced by 45%. Liquid solubility of the gases varies as shown in Table 5.3.

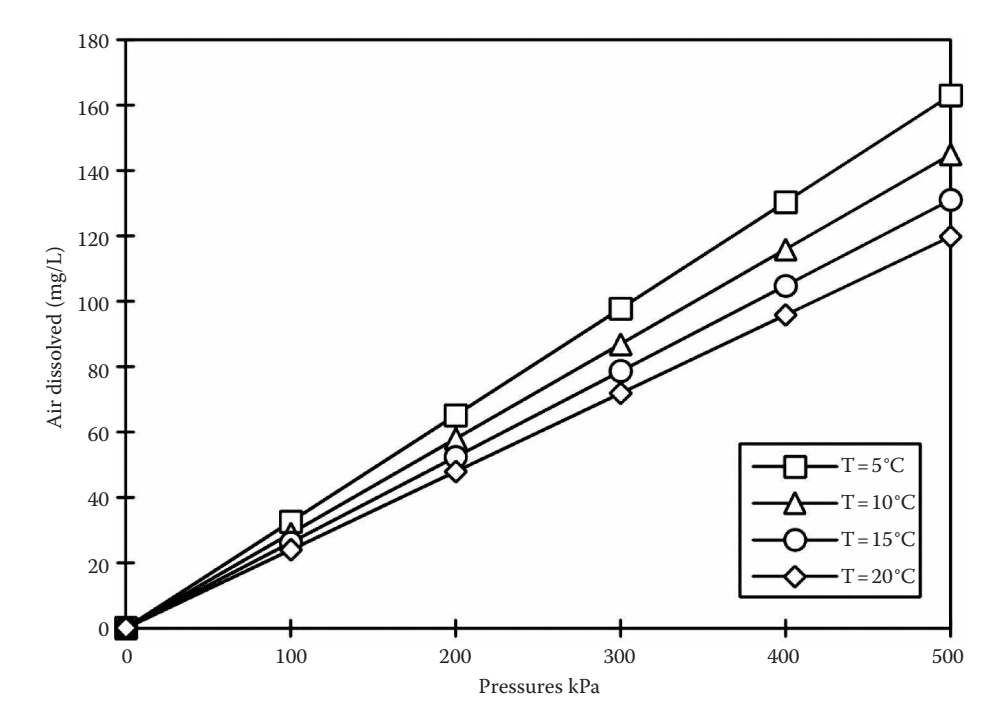


**FIGURE 5.9** Solubility of air in water. (From Adlan, M.N., A study of dissolved air flotation tank design variables and separation zone performance. PhD thesis, University of Newcastle Upon Tyne, 1998.)

TABLE 5.3 Solubility of Various Gases at 20°C and 760 mm Hg

Type of Gas	Cubic cm Gas/Cubic cm Water	Gram of Gas/100gm of Water
Nitrogen	0.015	0.0019
Oxygen	0.031	0.0043
Hydrogen	0.018	0.00016
Carbon dioxide	0.88	0.17
Carbon monoxide	0.023	0.0028
Air	_	1.87
Hydrogen sulfide	2.58	0.38
Sulfur dioxide	39.4	11.28

Source: Vrablik, E.R., Proceedings of the 14th Industrial Waste Conference, Purdue University, West Lafayette, IN, 743–779, 1959. Bratby and Marais in their studies on saturator performance indicated that it would be difficult to achieve full saturation at a saturator pressure <350 kPa [60]. From an economic point of view, the efficiency of the saturator system was important. They found that by using a packed system of 0.5 m depth with Raschig rings of 25 mm diameter, full saturation was achieved at saturator pressures beyond 250 kPa for a surface loading up to 2500 m/day. A similar level of saturation was found by Zabel and Hyde using a packed saturator of 0.75 m depth with 25 mm Berl saddles [23].

For design purposes, Bratby and Marais suggested that at a temperature of 20°C with a pressure of 3 atm., the concentration of air precipitated on reducing the pressure to atmospheric pressure is given by the following equation [60]:

$$a_{\rm P} = 19.5 \, p \, (\text{mg/L}),$$
 (5.19)

where p is the saturator pressure in atmospheres.

## 5.4.6 Bubble Generation

Rykaart and Haarhoff indicated that the geometrical design and operating conditions of the injection nozzles were important determining factors for bubble size [61]. They reported that saturator pressure does not have a consistent effect on nozzle efficiency. There were contradicting claims regarding whether a higher pressure produces smaller bubbles [55,62] or bigger bubbles [52,63]. But Jones and Hall reported that there was no significant relationship between pressure variation and bubble size [64].

Studies by Bratby and Marais [65] showed that the shape and roughness of the valve, the degree of turbulence and dilution of saturator feed downstream of the valve, and the concentration of particulate nuclei in the dilution water had a negligible effect on the precipitation of air from a solution (i.e., mass of air precipitated to unit volume of saturator feed). However, these findings were contradicted by those reported by others [55,61] in terms of the shapes and roughness of the valves. Rykaart and Haarhoff showed that at a saturator pressure of  $500\,\mathrm{kPa}$ , a nozzle with a bend in its channel produced a bubble size of  $49.4\,\mu\mathrm{m}$  (median diameter) compared with a nozzle with a tapering outlet that produced  $29.5\,\mu\mathrm{m}$  [61]. When the saturator pressure was reduced, the bubble sizes were reduced.

For a continuous-flow DAF plant, Edzwald and Walsh predicted that the concentration of air released in the tank  $(C_r)$  would be as follows:

$$C_{\rm r} = \left[ \left( \frac{C_{\rm S} - C_{\rm a}}{1 + R_{\rm r}} \right) \right] R_{\rm r} - K, \tag{5.20}$$

where  $C_a$  is the concentration of air that remains in solution at atmospheric pressure,  $R_r$  is the recycle ratio, which is equal to the recycle flow rate divided by the influent flow rate, and K is the influent saturation factor defined as  $(C_S - C_a)$ , where  $C_o$  is the concentration of air in the influent water. In most cases,  $C_o$  is saturated, and this means K = 0. To find the bubble volume concentration  $(\phi_b)$ , Edzwald and Walsh suggested that  $C_r$  be divided by the saturated density of air  $\rho_{sat}$  as shown in the following equation,

$$\phi_{\rm b} = C_{\rm r}/\rho_{\rm sat} \tag{5.21}$$

To get the generated air volume at the same temperature under atmospheric pressure, Takahashi et al. used the following equation by considering air as an ideal gas [55]:

$$V_{\rm A} = \left(\frac{\rho_{\rm w}}{M_{\rm w}}\right) \left(\frac{P_{\rm A} - P_{\rm O}}{P_{\rm O}}\right) \frac{RT}{H_{\rm E}},\tag{5.22}$$

where  $\rho_w$  is the density of water in gm/cm<sup>3</sup>,  $P_A$  is the dissolved pressure in dyne/cm<sup>2</sup>,  $P_O$  is the atmospheric pressure in dyne/cm<sup>2</sup>,  $P_O$  is the gas constant in erg/k · mol,  $P_O$  is the absolute temperature in Kelvin,  $P_O$  is the molecular weight of water in g/g·mol, and  $P_O$  is Henry's law constant in dyne/cm<sup>2</sup>.

By assuming that all the dissolved air in water changes into bubbles, the theoretical generated flow rate can be obtained using Equation 5.18. The experimental results by Takahashi et al. showed that the generated air flow rate increased with an increase in dissolved pressure and also with an increase in liquid flow rate [55]. To obtain the volume of air occupied by a single spherical bubble,  $V_b$ , Takahashi et al. suggested the following equation:

$$V_{\rm b} = \left(\frac{P_{\rm O} + \rho_{\rm w} g h + 4\sigma/d_{\rm av}}{P_{\rm O}}\right) \frac{\pi}{6} d_{\rm av}^3, \tag{5.23}$$

where h is the depth from the liquid surface to the bubble in cm,  $\sigma$  is the surface tension in dyne/cm<sup>2</sup>, and  $d_{av}$  is the volumetric mean diameter of the bubble in cm. According to the authors, the effect of liquid depth is negligible; thus, the measurement of the bubble diameter was carried out at the top of the flotation tank. The number of bubbles generated per cm<sup>3</sup> of water could be obtained from the following equation:

$$N_{\rm b} = \frac{G/Q}{V_{\rm b}},\tag{5.24}$$

where G is the volumetric flow rate of air generated under decrease in pressure (cm³/s), and Q is the volumetric flow rate of liquid (cm³/s). Their experimental results showed that by increasing the dissolved pressure and liquid flow rate, the number of bubbles will be increased. The geometry of the nozzle also affects the bubble size. By using a needle valve, Takahashi et al. obtained the following equation:

$$N_{\rm b} = 1 \times 10^4 \left( \frac{P_{\rm A} - P_{\rm O}}{P_{\rm O}} \right)^2 Q. \tag{5.25}$$

The calculated and experimental values of the number of bubbles were compared, and the results were claimed to be remarkably in agreement with the equation used.

For an efficient solid–liquid separation process, small bubbles are needed [66–68]. Bubble sizes in the range of  $20-80\,\mu m$  are capable of good attachment to floc particles. Larger bubbles will create a hydraulic disturbance along their rising path toward the surface and a decrease in the surface area. For example, a 2 mm bubble contains the same amount of air as 64,000 bubbles of 50  $\mu m$  in size. Collin and Jameson reported that the optimum bubble size in the microflotation process is approximately  $50\,\mu m$  [67].

## 5.4.7 Collision

Reay and Ratcliff, in their study of dispersed air flotation, defined the collection efficiency of a bubble as the fraction of particles in the bubble's path that are picked up by the bubble [69]. Particles of about  $3 \, \mu m$  diameter or larger will not be affected by Brownian motion. They will be in contact with the bubble only if their hydrodynamically determined trajectories come within one particle radius ( $r_p$ ) of the bubble. This region is called the collision regime. By considering the collision regime in which the Brownian diffusion is negligible [70], the collection efficiency of a bubble can be expressed as:

$$\eta = \eta_1 \times \eta_2, \tag{5.26}$$

where

 $\eta_1$  = collision efficiency, that is, the fraction of particles in the bubble's path that collided with the bubble

 $\eta_2$  = attachment efficiency, that is, the fraction of particles colliding with the bubble that stick to it

Equation 5.26 indicates that  $\eta_2$  will depend mainly on the chemical nature of the particle surface, the bubble surface, and the thin film of liquid draining from between them. Reay and Ratcliff also reported on the predicted collision efficiency and illustrated it with a graph;  $\eta_1 = 1.25 (r_p/R_b)^{1.9}$  for  $(\rho_p/\rho_f) = 1$ ,  $\eta_1 = 3.6 (r_p/R_b)^{2.05}$  for  $(\rho_p/\rho_f) = 2.5$ , and  $\eta_1$  is roughly proportional to  $(r_p/R_b)^2$  over the density range used. The symbols used in the aforementioned expressions are as follows [69]:

```
r_{\rm p} = particle radius (cm)

R_{\rm b} = bubble radius (cm)

\rho_{\rm p} = particle density (gm/mL)

\rho_{\rm f} = fluid density (gm/mL)
```

Since  $\eta_1$  is proportional to  $R_b^2$ , the average number of particles picked up by a bubble (by assuming  $\eta_1$  is constant) should be roughly independent of bubble size and the flotation rate should be proportional to bubble frequency (i.e., the amount of bubbles rather than bubble diameter over the entire range of particle sizes). This prediction is applicable to bubbles of diameter up to 0.1 mm [71]. However, when latex particles (3–9  $\mu$ m) having almost the same density as water and larger zeta potential (+10.6 mV) were used in the experiments, they could not get close to the bubble surface [71]. This means the bubble–particle collision model is not appropriate for latex particles.

Flint and Howarth, in their review on the collision efficiency of small particles with spherical air bubbles, reported that the collision of a particle with a bubble would depend on the balance of viscous, inertial, and gravitational forces acting on the bubble [72]. Besides that, the form of streamlines around the bubble also play an important role in whether or not collision takes place. Flint and Howarth formulated an equation of motion of a small spherical particle similar to a spherical bubble rising in an infinite pool of liquid in the *j*th direction as follows [72]:

$$m_{\rm p} \frac{av_j}{at} = G_j + C_{\rm d} \left( u_j - v_j \right), \tag{5.27}$$

where

 $G_j$  = body force acting on the particle; for raindrop collision,  $G_j$  = 0. In flotation, there is clearly a component of relative acceleration due to gravity because the bubble and particle are of distinctly different densities.

 $C_{\rm D}$  = dimensional drag coefficient for the particle, depending on the shape of the particle and the Reynolds number past it. For a spherical particle, the drag will be the same in all directions.

 $V_i$  = particle velocity.

 $u_j$  = velocity the fluid would have at the position of the particle if no particle were there. For fine particles in flotation, it is assumed that the flow around the particle has an insignificant effect compared with the flow pattern due to the bubble;  $u_j$  then depends on the shape of the bubble and the Reynolds number around it.

4t = time

By considering the relative two-dimensional motion of a spherical bubble and particle where the bubble is held stationary at the origin of the coordinate system by a liquid flow equal to the bubble

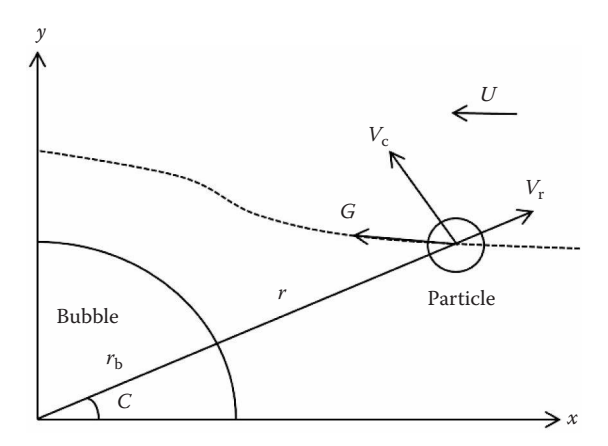


**FIGURE 5.10** Geometry of bubble–particle system. (From Adlan, M.N., A study of dissolved air flotation tank design variables and separation zone performance. PhD thesis, University of Newcastle Upon Tyne, 1998.)

rise velocity in the negative direction (Figure 5.10), Flint and Howarth suggested the equation of motion for the particle as follows [72]:

$$\frac{4}{3}\pi r_p^3 \rho_p \frac{\partial v_y}{\partial t} = 6\pi \mu_f r_p \left( u_y - v_y \right) \tag{5.28}$$

$$\frac{4}{3}\pi r_{p}^{3} \rho_{p} \frac{\partial v_{x}}{\partial t} = \frac{4}{3}\pi r_{p}^{3} \left(\rho_{p} - \rho_{f}\right) g - 6\pi r_{p} \left(u_{x} - v_{x}\right). \tag{5.29}$$

Reducing these equations to their dimensionless form and introducing the variable v, u, and t, and parameters K and G:

$$v_x^* = \frac{v_x}{u} v_y^* = \frac{v_y}{u}$$
$$u_x^* = \frac{u_x}{u} u_y^* = \frac{u_y}{u}$$
$$t^* = \frac{tu}{r_b}$$

and,

$$K = \frac{2\rho_{\rm p} r_E^2 u}{9\mu_{\rm f}} r_{\rm b}$$
$$G = 2\left(\rho_{\rm p} - \rho_{\rm f}\right) r_{\rm p}^2 \frac{g}{9\mu_{\rm f}} u$$

i.e.,

$$K \frac{\partial v_y^*}{\partial t^*} = u_y^* - v_y^*$$
$$K \frac{\partial v_x^*}{\partial t^*} = -G - u_x^* + v_x^*$$

where

 $r_p$  = particle radius (cm)

 $\rho_p$  = particle density (gm/mL)

 $\rho_f$  = fluid density (gm/mL)

v = component of particle velocity (cm/s)

t = time (s)

 $\mu_f$  = fluid viscosity (kg/m/s)

u = component of velocity field due to bubble (cm/s)

x, y = Cartesian position coordinates (cm)

v = dimensionless component of particle velocity (cm/s)

t =dimensionless time (s)

K = particle inertia parameter

G = dimensionless settling velocity of particle (cm/s)

According to Flint and Howarth, calculation for K down to 0.001 shows that the collision efficiency remains substantially constant for 0.001 < K < 0.1, meaning that collision efficiency is virtually independent of K and of whether Stokes or potential flow is assumed [72]. They suggested that for a fine particle characterized by K < 0.1, inertial effects of the particle may be neglected, and single bubble collision efficiency  $\eta$  can be calculated from:

$$\eta = \frac{G}{(1+G)}.$$
(5.30)

However, Flint and Howarth indicated that in the flotation tank, the collision efficiency may be several times as great as those predicted from single bubble calculations [72]. This may be due to at least three reasons:

- 1. The presence of hindering effects of the neighboring bubbles that reduced the rising velocity of the bubble. For fine bubbles, this could lead to an increase in collision efficiency.
- 2. Difference in the shape of liquid streamlines around the bubble. The greater the number of bubbles, the closer the assemblage and straighter the streamlines. This results in the increase of collisions between particles and bubbles.
- 3. The motion of particles upstream from the target bubble is influenced by the layers of bubbles ahead and is thus no longer parallel to the direction of bubble motion.

The aforementioned opinion, which was expressed by Flint and Howarth, is found to be in agreement with that of Fukushi et al., as the latter showed that a single collector collision model was not appropriate in the DAF process [45]. Furthermore, King indicated that the calculated collision efficiency based on the works of Reay and Ratcliff, Flint and Howarth, and Sutherland and Woodburn et al. were not in agreement with each other [73,71–72,74–75].

#### 5.4.8 Interception and Diffusion

According to Yao et al., a single particle of filter media is a collector, and if any suspended particle is in contact with the collector, then a process known as interception occurs [75]. The contact efficiency of a single media particle or collector is the ratio of the rate at which the particles strike the collector to the rate at which particles flow toward the collector, which can be expressed as follows:

$$\eta = \frac{\text{Rate at which particles strike the collector}}{u_o c_o \left(\frac{\pi d^2}{4}\right)},$$
(5.31)

where

 $u_0$  = water velocity (m/s)

 $c_{\rm o}$  = suspended particle concentration upstream from the collector where the flow is undisturbed by the presence of the grain

d = grain diameter (cm)

In the case of flotation, the single collector efficiency ( $\eta$ ) may be defined as follows [46,77]:

$$\eta = \frac{\text{Particle} - \text{buble collision rate}}{\text{Particle} - \text{bubble approach}}.$$
(5.32)

Reay and Ratcliff indicated that submicron particles will reach the bubbles mainly by Brownian diffusion. In the diffusion regime, collection efficiency will decrease with increasing particle radius,  $r_p$  [69]. Flotation of these submicron particles could be improved if they were agglomerated into flocs of suitable size in the collision regime. Theoretical calculations were made on particles with diameter <  $0.2 \,\mu m$  and bubbles size of  $75 \,\mu m$ . At normal temperatures and pressures, particles <1  $\,\mu m$  in diameter suspended in gases or water will exhibit a Brownian motion that is sufficiently intense to produce collision with a surface immersed in the fluid [78]. Yao et al., in describing basic transport mechanisms in water filtration, explained that when a particle in suspension is subjected to random bombardment by molecules of the suspending medium, then a Brownian movement of the particle known as diffusion takes place [76]. Numerical and analytical determinations of single-collector efficiency were discussed by Yao et al. based on the works of previous investigators, and the following equations were established:

$$\eta_{\rm D} = 4.04 \,\mathrm{Pe}^{-2/3} = 0.9 \left(\frac{kT}{\mu d_{\rm p} dv_{\rm o}}\right)^{2/3}$$
(5.33)

$$\eta_{\rm I} = \frac{3}{2} \left( \frac{d_{\rm p}}{d} \right)^2 \tag{5.34}$$

$$\eta_{\rm g} = \frac{(\rho_{\rm p} - \rho)}{18\mu v_{\rm o}} g d_{\rm p}^2,$$
(5.35)

where  $\eta_D$ ,  $\eta_I$ , and  $\eta_G$  are the theoretical values for single-collector efficiency when the sole transport mechanisms are diffusion, interception, and gravity settling, respectively. Pe is the Peclet number (i.e.,  $Pe = 2R_bU_b/D_f$ , where  $R_b$  is bubble radius,  $U_b$  is bubble rising velocity, and  $D_f$  is particle diffusivity in cm<sup>2</sup>/s), k is Boltzmann's constant, T is the absolute temperature,  $d_p$  is the diameter of suspended particle, d is the diameter of the collector or the bubble, which is equal to  $d_p$ ,  $v_o$  is the approach velocity of fluid, and  $\rho$  is the density of fluid, which is equal to  $\rho_f$ .

Then the expression for total single-collector efficiency of a media grain can be written as follows [76,79]:

$$\eta_{\mathrm{T}} = \eta_{\mathrm{D}} + \eta_{\mathrm{I}} + \eta_{\mathrm{G}}.\tag{5.36}$$

Edzwald and Walsh used the same theoretical approach as in filtration to develop a conceptual model for flotation [10,76,79]. Thus, the following equations are introduced:

$$\eta_{\rm D} = 0.9 \left( \frac{k_{\rm b} T}{\mu d_{\rm p} d_{\rm b} U_{\rm b}} \right)^{2/3} \tag{5.37}$$

$$\eta_{\rm I} = \frac{3}{2} \left( \frac{d_{\rm p}}{d_{\rm b}} \right)^2 \tag{5.38}$$

$$\eta_{G} = (\rho_{p} - \rho_{f}) \frac{gd_{p}^{2}}{18\mu U_{b}}.$$
(5.39)

Comparing the equations used in filtration to the aforementioned equations, the approach velocity of fluid and Boltzmann's constant have been changed to  $U_b$  (bubble rise velocity) and  $k_b$  (Boltzmann's constant for bubble), respectively. This is done to suit the mechanisms involved in flotation. Ward, in his review on capture mechanisms, introduced a new form of equations for  $\eta_D$  and  $\eta_G$  by substituting the bubble rise velocity U from Equation 5.4 into Equations 5.37 and 5.39. Thus, we have the following result [56]:

$$\eta_{\rm D} = 6.18 \left( \frac{kT}{\rho_{\rm f} g d_{\rm p}} \right)^{2/3} \left( \frac{1}{d_{\rm b}} \right)^2 \tag{5.40}$$

$$\eta_{\rm G} = \left(\frac{d_{\rm p}}{d_{\rm b}}\right)^2 \frac{\left(\rho_{\rm p} - \rho_{\rm f}\right)}{\rho_{\rm f}}.\tag{5.41}$$

Results on single-collector efficiency by Edzwald and Walsh show a minimum efficiency occurs at a particle size of around 1 µm [10]. For removal efficiency, Edzwald et al. used the same principle as in Equation 5.26, changing only the symbols of the expression as follows:

$$R = \alpha_{\rm E} \eta_{\rm T} (100\%),$$
 (5.42)

where  $\alpha_E$  is the attachment efficiency. If the total number of bubbles ( $N_b$ ) is considered, then Edzwald et al. suggests the following equation for particle removal:

$$\frac{\mathrm{d}N_{\mathrm{p}}}{\mathrm{d}t} = -\left(\alpha_{\mathrm{pb}}\eta_{\mathrm{T}}\right)A_{\mathrm{b}}U_{\mathrm{b}}N_{\mathrm{b}}N_{\mathrm{p}},\tag{5.43}$$

where  $A_b$  is the projected area of the bubble and  $N_p$  is the particle number concentration. By having a bubble volume concentration of  $\Phi_b = \pi d_b^3 N_b/6$ , and substituting into Equation 5.43, we have the following equation:

$$\frac{dN_{p}}{dt} = -\left(\alpha_{pb}\eta_{T}\right)\frac{\pi d_{b}^{2}}{4}U_{b}N_{p}\frac{6\Phi_{b}}{d_{b}^{3}} = -\left(\frac{3}{2}\right)\left(\frac{\alpha_{pb}\eta_{T}U_{b}\Phi_{b}N_{p}}{d_{b}}\right). \tag{5.44}$$

The particle number concentration removal in terms of flotation tank depth can be rewritten as:

$$\frac{\mathrm{d}N_{\mathrm{b}}}{\mathrm{d}H} = -\frac{3}{2} \left( \frac{\alpha_{\mathrm{pb}} \eta_T \Phi_{\mathrm{b}} N_{\mathrm{p}}}{d_{\mathrm{b}}} \right). \tag{5.45}$$

Edzwald et al. also produced a summarized table of their model parameters for DAF facilities. This is as shown in Table 5.4. However, this model has not been tested or verified [10].

TABLE 5.4
Model Parameters for DAF Facilities

Parameter	Affected by	Comments			
	Pre Treatment				
$\alpha_{pb}$ (particle-bubble attachment efficiency)	Particle-bubble charge interaction and hydrophilic nature of particles	Improve $\alpha_{pb}$ by chemical pretreatment, coagulation, and pH conditions			
$N_{\rm p}$ (particle number concentration)	Coagulation addition and flocculation time	Coagulant may add particles, flocculation may reduce $N_p$ and increase $d_p$ .			
$\eta_T  (\text{single collector efficiency})$	Diffusion and interception	Minimum for $d_p$ of 1 $\mu$ m			
Flotation Tank					
$d_{\rm p}$ (bubble diameter)	Saturator pressure	Small bubbles produce large interfacial areas and surface forces between bubbles and particles. Small bubbles, improve $\eta_T$			
$\Phi_{\rm b}$ (bubble volume concentration	Saturator pressure and recycle ratio	Large $\Phi_b$ ensures collision opportunities and lowering of floc density			

Source: Edzwald, J.K., Walsh, J.P., Dissolved air flotation: Laboratory and pilot plant investigation. AWWA Research Foundation and AWWA, 1992.

Ward, in his article on DAF, made an improvement on Equation 5.45 by integrating it over the tank depth H from  $N = N_0$  at the surface H = 0 to N = n at the tank base H = H. Thus, the overall particle removal equation becomes [56]:

$$N = N_o e^{-\left(\frac{3\alpha_{\rm pb}\eta_T \Phi_b H}{2d_b}\right)}.$$
 (5.46)

Then, the overall efficiency is given by:

$$\eta = 1 - \frac{N}{N_0}. (5.47)$$

## 5.4.9 TANK DESIGN

The usual design procedure for any flotation unit can be based on Figure 5.11. All the suspended solids in the flotation chamber should have a sufficient rise velocity to travel the effective depth D within the specified detention time T. This means the rise rate  $V_T$  must be at least equal to the effective depth D divided by the detention time T, or equal to the flow divided by the surface area:

$$V_{\rm T} = \frac{D}{T} = \frac{Q}{A_{\rm S}},\tag{5.48}$$

where

 $V_{\rm T}$  = vertical rise rate of suspended solids (m/s)

D = effective depth of flotation chamber (m)

T = detention time (s)

 $Q = \text{influent flow rate, } (\text{m}^3/\text{s})$ 

 $A_{\rm S}$  = surface area of flotation chamber (m<sup>2</sup>)

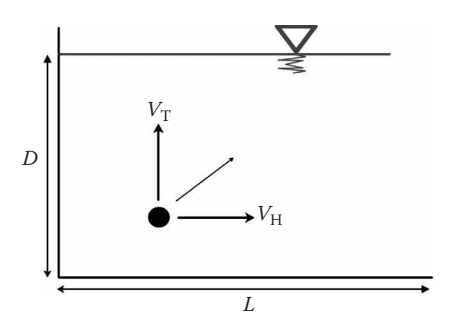


**FIGURE 5.11** Basic design concept of flotation unit. (From Adlan, M.N., A study of dissolved air flotation tank design variables and separation zone performance. PhD thesis, University of Newcastle Upon Tyne, 1998.)

The particles to be removed must also have a horizontal velocity

$$V_{\rm H} = \frac{Q}{A_{\rm C}},\tag{5.49}$$

where

 $V_{\rm H}$  = horizontal velocity (m/s)

 $A_C$  = cross-sectional area of flotation chamber (m<sup>2</sup>)

If the flotation chamber is in a rectangular shape, then the following equations can be established:

$$W = \frac{A_{\rm C}}{D} \tag{5.50}$$

$$L = \frac{A_{\rm S}}{W} = \frac{A_{\rm S}}{(A_{\rm C}/D)} = V_{\rm H} D \frac{A_{\rm S}}{Q}, \tag{5.51}$$

where

W is the width of the flotation chamber (m),

L is the effective length of the flotation chamber (m),

Q is the influent flow rate  $(m^3/s)$ ,

and the value of D/W is usually between 0.3 and 0.5.

The size of the flotation tank can be reduced if the separation rate is increased [80]. Katz and Wullschleger showed that a particle with a bubble attached to it would increase in its rising rate with an increase in the particle size. This finding is similar to that reported by Packham and Richards [38]. However, other factors such as pressure, recycle ratio, temperature, pH, zeta potential of the particles, number and size of bubbles produced, types of nozzles, flocculation process, flow condition, and configuration of the tank are believed to have a significant effect on the separation process [11,45,81].

Longhurst and Graham reported that the surface overflow rate (SOR) or rise rate is the fundamental criterion for tank design [15]. It is defined as the flow rate divided by the surface area of the flotation tank. In practice, the surface area is based on the interfacial area between clarified water and sludge, and not on the total area of the flotation tank [15]. The characteristics of water and bubble size will determine the air/floc aggregate rise velocity. For normal design purposes, rise velocities between 3 and 8 m/h have been used [68]. For laminar flow, the maximum size of bubbles is 130 µm; for bubbles measuring <130 µm, Stokes' law applies [11], and Equation 5.2 can be

HK

used to calculate the rise rate. The maximum bubble size for laminar flow can be calculated using Equation 5.3 by assuming limited laminar flow, Re = 1, and using the relationship between bubble size and rise rate of air bubble, which has been established in graphical form [11]. A survey carried by Longhurst and Graham showed that the average normal operating SOR is below 6–9 m/h with a maximum rate of up to 11 m/h [15].

Bratby and Marais, in their investigation on the application of DAF in activated sludge, were of the same opinion as Longhurst and Graham regarding the design of flotation units [15,82]. Instead of SOR, Bratby and Marais used the term down flow rate, which is defined as the total flow into the unit divided by the plan area at the outlet. It is the value of limiting down flow rate ( $V_L$ ), where the bubble–particle agglomerates are carried down with the effluent that controls the design of the tank. Data published by Edzwald on the design and operation parameters of DAF showed that there were still considerable variations in retention time, hydraulic loading, and recycle ratio between different treatment works in different parts of the world [83]. These are shown in Table 5.5.

In terms of shape, Zabel and Melbourne indicated that a rectangular shape has gained greater acceptance due to advantages such as simple design, easy introduction of flocculated water, easy

TABLE 5.5
Summary of DAF Design and Operation Parameters

D (	6 4 46 1	e: 1 1	The state of the s	1.11/	UK	c !: ·
Parameter	South Africa	Finland	The Netherlands	UK	(Edzwald)	Scandinavia
			Flocculation			
Intensity						
Time (min)	4–15	20-127	8–16	20-29	18-20	28-44
			Flotation			
Reaction zone						
Time (min)	1–4		0.9-2.1			
Hyd. load. (m/h)	40-100		50-100			
Separation zone						
Hyd. load. (m/h)	5-11	2.5-8	9–26			
Total flotation area						
Hyd. load. (m/h)			10–20	5–12	8.4–10	6.7–7
Time (min.)					11-18	
Recycle (%)	6–10	5.6-42	6.5–15	6-10	5-10	10
			Unpacked Sat.			
Pressure (kPa)	400-600		enpaenea san		400-550	460-550
Hyd. load. (m/h)	20-60					
Time (s)	20-60					
			D 1 10 (			
D (1-D-)	200 (00		Packed Sat.		400 500	
Pressure (kPa)	300–600				400–500	
Hyd. load. (m/h)	50–80					
Packing depth (m)	0.8–1.2					
			Saturators			
Pressure (kPa)		300-750	400-800	310-830	480–550	

Source: Edzwald, J.K., Water Sci. Technol., 31, 1-23, 1995.

<sup>&</sup>lt;sup>c</sup> Unspecified with respect to unpacked or packed saturator, [1,2,15,83].

float removal, small area, and flexibility of scale-up [21]. In addition to that, floc breakup is minimized, hydraulic efficiency is maximized, and engineering and construction is simplified [15]. A tank with SOR in the range 6–12 m/h would have a depth of 1.2–1.6 m and a residence time of 5–15 min [84]. Results from a survey (questionnaire) carried out by Longhurst and Graham in Great Britain showed that, in practice, tank depths range 1–3.2 m with a mean value of 2.4 m, while tank shapes vary from "squarish" to "long and thin"; however, there is a continuing debate in this area [15]. Gregory and Zabel indicated that tank depth of about 1.5 m with an overflow rate of 8–12 m/h (depending on the type of water) is normally used [11]. An effective flotation unit could be between 0.48 and 2.74 m deep [6]. The angle for the inlet baffle is approximately 60° to the horizontal, which ensures minimum disturbance to the bubble–floc agglomerate [18]. However, Longhurst and Graham reported that, in theory, the baffle angle can range from 45° to 90° to the horizontal [15]. "Purac" have used a vertical baffle in the production of the "Flofilter" tank to avoid an eddying current during clarification and hydraulic congestion during filter backwash. But for the conventional filter, they preferred to use an inclined baffle.

The depth of water below the water surface is found to vary across treatment plants, and greater depths than those recommended by the Water Research Centre of 0.3–0.4 m are normally used [15]. In South Africa, the depth varies from 1.5 to 3.5 m, and in the United Kingdom it varies from 1.0 to 3.2 m [85]. This means there is still no agreement about the extent to which depth affects the optimization of design criteria. Regarding the width of the tank, it was observed that widths between 2.4 and 9.4 m are found in practice. However, Gregory and Zabel reported that tank widths are less significant to hydraulic flow and are sometimes restricted by the sludge-removing device [11]. A study carried out by Heinanen on the use of DAF for potable water treatment in Finland showed that the design parameters for the process are still far from ideal and this has resulted in high construction costs [14]. He indicated that the situation could be avoided if research institutes had played an important part in the design work.

Discussions with Noone [82] indicated that there is a need to investigate the optimum shape of the tank. This means further investigations would be useful to justify the arrangements of the nozzles, the distance between the inlet and the baffle, the baffle angle, and the depth of water surface from the baffle. Longhurst and Graham indicated that if the length of the tank runs only up to point A (Figure 5.12), the tank may be too short, and the floc will not achieve its optimum flotation that occurs at point B [15,87]. At point C, the tank is too long, which will cause the floc to settle down.

Noone indicated that even in Severn Trent Water, there is a range of tank sizes with varying rectangular shapes and different arrangements of air nozzles, baffles, depths, and operational

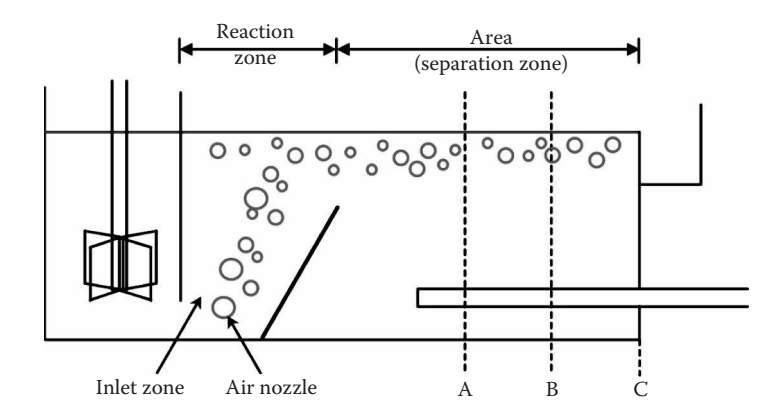


**FIGURE 5.12** Arrangements in flotation tank. (From Adlan, M.N., A study of dissolved air flotation tank design variables and separation zone performance. PhD thesis, University of Newcastle Upon Tyne, 1998; Murshed, M.F., Removal of turbidity, suspended solid and aluminum using DAF pilot plant. MSc thesis, Universiti Sains Malaysia, 2007.)

procedures, with no evidence to prove their effectiveness [82]. Thus, it is worth investigating these parameters so that a better fundamental understanding can be developed regarding the optimization of tank dimensions and the flotation process in practice. This could result in the saving of power, chemicals, and operation times and in the development of standard design procedures.

Based on the comments by Noone, Adlan had carried out investigations at several water treatment plants belonging to Severn Trent Water [88]. Acoustic Doppler Velocimeter with three-dimensional down-looking probe was used in the investigation as it is ideal for measuring velocity close to the bottom of the boundary layer. Turbidity data were monitored at the same points where velocity data were taken in the separation zone of DAF tanks. Comparisons were made, and results showed that the design of the rectangular DAF tank could be improved by reducing the length of the separation zone without reduction in turbidity.

## 5.5 ADVANTAGES OF DAF APPLICATION IN WASTEWATER TREATMENT

The flotation technique has distinctive advantages over the conventional gravity settling technique for the removal of low-density particles that have a tendency to float. Flotation techniques are classified based on the methods of producing bubbles. The advantages of DAF are as follows [23,89–91,106–108]:

- Efficient at removing particles and turbidity, resulting in more economical filter designs. It allows short detention time of about 5–10 min in flocculation tanks.
- Higher hydraulic loading rates can be used than in most settling processes.
- More efficient than sedimentation in removing low-density floc formed from coagulation of Total Organic Compound (TOC).
- It allows lower coagulant dosages resulting in smaller chemical storage and lesser sludge.
- · Smaller footprints with stacked flotation over filtration arrangement.
- · Improved algae removal and cold water performance.
- · Less sensitive to flow variations.
- Process flexibility through air loading.

## 5.6 APPLICATION OF DAF PROCESS IN WASTEWATER TREATMENT

DAF process is a physical process which has been used widely in wastewater treatment. DAF is generally used as a combination process with coagulation. The industries that implement DAF for their wastewater treatment process are paper mill, chemical-mechanical polishing (CMP) wastewater, meat industry, personnel care product, and seafood industry [5,92–95]. Oily wastewater or oil refineries wastewater also use DAF for their wastewater treatment [90,97–101].

Zoubolis and Avranas applied coagulation and DAF process in treating simulated oily wastewater (using octane) with an initial concentration of 500 mg/L [96]. The coagulants used in this study were anionic polyacrylamide, cationic (K-1384), and FeCl<sub>3</sub>. Sodium oleate (NaOl) was used as a collector. It is a common anionic flotation collector used to enhance the floatability of coagulated solids and emulsion droplets (flotation collector). The DAF system was operated as a batch study using DAF jar-test with a pressure of 4–5 atm. and recycle ratio of 30%. Results indicated that the use of polyacrylamide and cationic (K-1384) did not offer a good solution. However, using FeCl<sub>3</sub> to demulsify and increase the droplets size improved the droplet–bubble adhesion and the overall DAF performance. The best removal rate for oil removal was obtained at 100 mg/L Fe<sup>3+</sup> with 50 mg/L NaOl at pH 6 and recycle ratio of 30%. The pH was optimum at 6 because at this pH, with the addition of Fe<sup>3+</sup>, the zeta potential of the hydrocarbon particle is nearly zero, and the electrostatic barrier is greatly reduced, which thus improves the droplet–particle attachment.

Al-Shamrani et al. carried out another study using DAF and coagulation in treating oily wastewater [25]. The study was carried out in a batch process. The sample was a solvent-refined petroleum distillate manufactured from crude petroleum oil. Alum was used as a coagulant agent at 100 mg/L with pH 8. The DAF system was equipped with a packed saturator column with 90% efficiency, and the recycle ratio was set at 10%. Two situations were observed in this study. First, at low concentration of alum with high working pressure for the saturator (80 psi) and high recycle ratio (20%), only 72% of oil was removed. However, increasing the dosage up to 100 mg/L at pH 8 with the same working pressure (80 psi) but at lower recycle ratio (8%), almost all the oil was removed. This finding shows that the increase in alum concentration destroyed the protective action created by the emulsifying agent (compound in oily wastewater). Simultaneously, the repulsive effects of the electrical double layers (zeta potential) were reduced as the concentration of alum increased. This results in the formation of larger droplets or particles through coalescence.

In 2003, Zouboulis et al. studied the removal of humic acid from synthetic landfill leachates as a possible post-treatment stage after biological treatment using coagulation and DAF [100]. This experiment used a column flotation. Samples were prepared with humic acid concentration from 50 to 300 mg/L, with 30% humic acid accounted for in the COD value. It means that after the biological treatment of the landfill leachate, the COD value ranges from 500 to 1000 mg/L, in which humic acids account for around 30%. This compound is a very reluctant organic acid. The coagulation process carried out prior to DAF used ethanol as frother and *N*-acetyl-*N*,*N*,*N*-trimethylammonium-bromide (CTAB) as a collector. The frother function is used to control the efficiency of bubble generation and to combine effectively with the collector. In the DAF system, the bubbles are produced by injecting air from the bottom of the column through a microporous frit at a flow rate of 200 cm<sup>3</sup>/min. According to Zouboulis et al., there are three main steps in the flotation mechanism:

- 1. Surface modification of the specific "species" (concerned compounds or contaminants) in the water or wastewater using chemicals.
- 2. Contact and adherence of hydrophobic species with bubbles.
- 3. Separation of particles.

In this study,  $70\,\text{mg/L}$  of collector was used with 5 min flotation time resulting in 95% humic acid removal. As a result, this study proved that the flotation process can be used as a post-treatment in the landfill leachate. Besides, they discovered the parameters that control this process: (1) type and dosage of frother, (2) dosage of collector, (3) pH solution, (4) ionic strength (concentration of other salt), and (5) flotation time. Studies conducted by other researchers dealt with all these parameters, except the ionic strength. In the study conducted by Zouboulis et al., two different salts were studied, the  $Na_2SO_4$  and NaCl [100]. Increasing the concentration of these salts above 0.01 M decreases humic acids removal. This proves that the ions  $(SO_4^{2-}$  and  $Cl^-)$  compete or interact with the cationic collectors. As a result, ions reduce the chances of humic acids to float. However, comparing  $SO_4^{2-}$  and  $Cl^-$ , the  $Cl^-$  effects are not significant and they decrease the overall percentage removal of humic acids to 10% only. This may be due to the charges carried by  $SO_4^{2-}$ , which is double, thus reacting more with the collector compared to  $Cl^-$  with one charge.

Another important point in this work is the zeta potential measurement at the optimum dosage. Results indicate that reduction in zeta potential (from negative value to zero) increases in percentage the removal of humic acids. However, beyond the optimum points, the results of zeta potential show the opposite charge (positive). This proves that to obtain a good agglomeration, the zeta potential of the concerned compound with collector or coagulant agent should be low or near zero.

Another study by Hami et al. showed the ability of coagulation and DAF in treating wastewater in refineries [98]. The sample was collected from the effluent of the American Petroleum Institute (API) separator. The coagulation process was carried out as a pre-treatment using a mixed coagulant containing alum, polyelectrolyte, and powered activated carbon (PAC). The suitable pH was in the range 6.5–8.0. The DAF process was carried out in a laboratory as a pilot scale. Three different pressures (2, 3, and 5 atm.) were chosen for this study, and the flow rate depended on the flow characteristics of pumps. For the DAF and recycle unit, the flow rate was 1.0–5.0 L/h and 1.0–2.0 L/h,

respectively. In the first phase of the study, the DAF process as a single treatment did not offer good COD and BOD removals. Only 19%–64% and 27%–70% of COD and BOD removals were, respectively, obtained using DAF alone. However, increase in percentage removal was achieved by a combination of coagulation and DAF. The COD and BOD removals were 72%–92.5% and 76%–94%, based on the initial concentration of 198 and 95 mg/L, respectively. Alum was believed to reduce the zeta potential of the particle in the influent, which thus provoked the agglomeration process, while the polyelectrolyte worked as a flocculant agent, and the PAC provided a site for the particles to absorb, and subsequently the floc was removed by flotation. Another factor that was addressed in this study was the flow rate through the nozzle in the flotation tank. Hami et al. found that the increase in flow rate causes a decrease in percentage removal because when high flow rate was applied, the resident was reduced (the bubbles do not have enough time to float all the particles). Owing to this, the amount of effluent with lower contaminant concentration was reduced, which resulted in low recycle ratio. Subsequently, it reduced the dispersed air bubbles due to lower gas holdup.

Tsai et al. utilized nano-bubble flotation to treat CMP wastewater [92]. The experimental works were carried out using laboratory and pilot scale experiments. The coagulants, also known as activators, used in this study were alum, ferric chloride, and PACL. The flocculant (collector) types utilized after the coagulation process were CTAB and NaOl. In the DAF system, a special equipment named NBG (nano-bubble generator) was used to produce the nano-sized bubble. The recycled water was injected into the flotation cell through NBG at pressure around 7.7 atm. The bubble size was around 30–5000 nm. Based on an experiment using the laboratory scale DAF unit, PACL performs better than alum. However, a combination of FeCl<sub>3</sub> with NaOl is superior to other combinations. Conversely, a combination of PACL-NaOl was used in the NBFT (nano-bubble flotation technology) as a pilot scale due to some advantages of PACL in terms of cost and chemical characteristics. Experimental results using the NBFT process show that chemical cost was reduced four times that of the conventional coagulation-sedimentation process. The addition of the collector shows that it is able to absorb at the air-liquid interface and enhance the resistance of the bubble to burst. The collectors provide an electrical potential to the bubble-particle and enhance the flotation process. Another advantage of adding a collector (NaOl in this study) is that it is able to reduce the bubble size, thereby increasing the flotation process. Moreover, the hydraulic retention time (HT), bubble size, bubble quantity, and saturator pressure considerably influenced the NBFT process. Based on this study, the optimum condition for NBFT process in treating the CMP wastewater was 50-60 mg/L of PACL and 5-10 mg/L of NaOl with 1 h HT, and 10%-20% recycle ratio. The pH was not adjusted, and the raw pH value was 9.4. More than 95% of turbidity, total solids, and total silica were removed.

de Nardi et al. focused on treating slaughterhouse wastewater using DAF process as laboratory and pilot plant scale experiments [93]. Coagulation process was carried out prior to DAF using PACL and anionic polyacrylamide. In the pilot plant scale experiment, the coagulation process used 24 mg Al<sup>3+</sup>/L PACL with 1.5 mg/L anionic polymer, followed by DAF process using 100% influent pressurization at 300 kPa. The lab-scale experimental process was conducted with and without coagulation. The concentration of the coagulant and flocculant was the same as that in the pilot scale experimental process. However, the pressure was higher compared with the pilot scale, which was 450 kPa. Another difference between pilot and laboratory scale processes in this study was the recycle ratio. In the laboratory scale experimental work, 40% recycle ratio was applied. Results indicated that using the pilot-scale full pressurization, the removal for Suspended solids (SS), oil and grease (O&G) was unsatisfactory at 28%–58% and 41%–57%, respectively. However, in a lab-scale setup with recycle ratio, the removal is higher than the pilot plant scale experiment. This could be due to the recycle ratio and pressure. As mentioned earlier, these two factors significantly affect the DAF efficiency in terms of the bubble size and bubble concentration. Comparison of DAF with and without coagulation in the lab-scale experimental setup showed that the combination of coagulation and DAF gave higher removal than DAF as a single process. Around 54%–60% and 46%–74% removals of SS and O&G, respectively, were obtained when using DAF as a single treatment, while a combination treatment (coagulation/DAF) gave 74% and 99% removal in their respective order. This proves that chemical treatment is very important for improving DAF performance. Recycle ratio is an important factor for boosting the removal efficiency. Recycle ratio is also efficient in controlling and varying the amount of air supplied.

de Sena et al. utilized coagulation/DAF as pre-treatment to treat the wastewater from the meat industry [94]. Ferric chloride with 80 mg/L Fe<sup>3+</sup> was used during the coagulation process, and the DAF process was operated at 4.0 bars, with 5 min saturation time and 20% recycle ratio. Application of coagulation/DAF in this study gave 60.5% and 78% removal of BOD<sub>5</sub> and COD from the initial concentration of 1500 and 2900 mg/L, respectively. This research work proves that this chemical or physical process can be used as a pre-treatment process.

Another application of DAF was carried out in treating personnel care product wastewater collected from Unilever Masheq Company, Egypt [95]. Comparison was made between coagulation or precipitation and coagulation/DAF. Three types of coagulants were tested. The coagulants concentration was 600, 800, and 700 mg/L, while the optimum pH was 8.23, 9.1, and 6.9 for ferric chloride, ferric sulphate, and alum, respectively. The DAF process was operated at 4.0 bars. The coagulation/precipitation process gave COD removal of around 75.8%, 77.5%, and 76.7% using ferric chloride, ferric sulphate, and alum, respectively, and the BOD<sub>5</sub> removals were 78%, 78.7%, and 74%, respectively. The coagulation or DAF process gives different outputs, such as differences in BOD removal. Using the three types of coagulants is not significant. However, the COD removals were 71.5%, 67.7%, and 77.5% for ferric chloride, ferric sulphate, and alum, respectively. This experimental study shows that the use of coagulation or DAF offers lower investment and running cost compared with coagulation or precipitation, around 27.3% and 23.7%, respectively. The application of DAF is summarized in Table 5.6.

## 5.7 APPLICATION OF DAF PROCESS IN LANDFILL LEACHATE TREATMENT

To date, the DAF is used more in industrial wastewater treatment for paper mill, meat processing, and oil-based industries like POME, soap and oil refinery industry. The performance of DAF in numerous research works has been summarized in Table 5.6. In 2000, Zouboulis et al. studied humic acid removal from simulated leachate using DAF process [96]. However, based on the literature review, no study has been carried out for actual landfill leachate treatment using DAF process. This indicates that there is a gap in the knowledge of DAF capability in leachate treatment. Based on the advantages offered by DAF, such as higher hydraulic loading, allowing lower coagulant dosages, being less sensitive to flow variations, and many more (described in Section 5.5), DAF process can be a good alternative for landfill leachate treatment. Recently, study on semi-aerobic landfill leachate treatment using DAF was carried out by Palaniandy et al. and Adlan et al. [101,102].

The study carried out by Palaniandy et al. suggests a way to apply this method as a large-scale application in landfill areas [101]. This research work investigates the application of DAF in leachate treatment with and without alum coagulation. Based on the study, a coagulation process must be introduced to facilitate the destabilization of colloidal particles or emulsions. This is because DAF process in leachate treatment without coagulation shows that the variations in percent removal of turbidity, color, and COD were considerably low, which implies that the main pollutant in the leachate was in soluble organic and inorganic matter such as humic acid, fulvic acid, iron, sodium, potassium, sulfate, and chloride, [102,103]. However, with the addition of coagulant (alum), the percentage removal of the studied parameters increased to 70%,79%, and 42% for color, COD, and turbidity, respectively. Based on this study, DAF process is able to treat landfill leachate. Further research has been carried out by Adlan et al. in this field by optimizing coagulation and DAF process in semi-aerobic landfill leachate using response surface methodology (RSM). In this research work, ferric chloride (FeCl<sub>3</sub>) was chosen to induce coagulation [102]. The results show 50%, 75%, 93%, and 41% reduction in turbidity, COD, color, and NH<sub>3</sub>–N, respectively. Comparing this research work

**TABLE 5.6 Summary of Previous Studies on DAF Process** 

Parameter Concern	Operating Parameter	Findings	Authors
Oil removal	<ul> <li>100 mg/L Fe<sup>3+</sup></li> <li>50 mg/L NaOl</li> <li>pH 6</li> <li>Saturator pressure 4–5 atm.</li> <li>Recycle ratio 30%</li> </ul>	Results indicate that the use of polyelectrolyte did not offer favorable results. However, using the FeCl <sub>3</sub> to demulsify and increase the size of droplets and improve the droplet–bubble adhesion, the overall DAF performance increased.	Zouboulis and Avranas [96]
Oil removal	<ul> <li>100 mg/L alum</li> <li>pH 8</li> <li>Saturator pressure (80 psi)</li> <li>Recycle ratio (20%)</li> <li>Packed saturator column with 90% efficiency</li> </ul>	Increase in alum concentration destroyed the protection action created by the emulsifying agent (compound in oily wastewater). Simultaneously, the repulsive effects of the electrical double layers (zeta potential) were reduced as the concentration of alum increased.	Al-Shamrani et al. [25]
Humic acid removal	<ul> <li>Ethanol as frother</li> <li>70 mg/L CTAB as a collector</li> <li>Bubbles were produced by injecting the air from the bottom of the column through a microporous frit, at a flow rate of 200 cm³/ min.</li> <li>5 min flotation time</li> </ul>	Removal of humic acid was 95%.  This study proves that the flotation process can be used as a post-treatment in landfill leachate.  Increasing the concentration of salts (SO <sub>4</sub> <sup>2-</sup> and Cl <sup>-</sup> ) above 0.01 M resulted in the decrease in humic acids removal.  Comparison between SO <sub>4</sub> <sup>2-</sup> and Cl <sup>-</sup> , the Cl <sup>-</sup> effects was not significant, and it decreased the overall percentage removal of humic acids, which was only 10%.  To obtain a good agglomeration, the zeta potential of the concerned compound with collector or coagulant agent should be low or near zero.	Zouboulis et al. [100]
COD and BOD from refineries wastewater	<ul> <li>Mixed coagulant contained alum, polyelectrolyte, and powered activated carbon (PAC).</li> <li>Suitable pH is in the range of 6.5 and 8.0.</li> <li>The flow rate depended on the flow characteristics of pumps; for DAF and recycle unit, the flow rate was 1.0–5.0 L/h and 1.0–2.0 L/h, respectively.</li> </ul>	19%–64% and 27%–70% removal of COD and BOD, respectively, using DAF alone.  Combination of coagulation and DAF, COD, and BOD removals were 72%–92.5% and 76%–94%, respectively, from the initial concentration of 198 and 95 mg/L, respectively.  The alum was believed to reduce the zeta potential of the particle in the influent; thus, it provokes an agglomeration process while the polyelectrolyte works as a flocculant agent; the PAC provided a place for the particles to adsorb, and subsequently the floc was removed by flotation.	Hami et al. [98]
			(Continued)

# TABLE 5.6 (*Continued*) Summary of Previous Studies on DAF Process

Parameter Concern	Operating Parameter	Findings	Authors
Turbidity, total solids, and total silica removal from CMP wastewater	<ul> <li>50–60 mg/L of PACL</li> <li>5–10 mg/L of NaOl</li> <li>1h HT</li> <li>10%–20% recycle ratio</li> <li>pH was not adjusted, and the raw pH value was 9.4</li> <li>NBG (nano bubble generator) was used to produce the nano-sized bubble.</li> <li>Pressure around 7.7 atm.</li> <li>Bubble size was around 30–5000 nm</li> </ul>	This study indicated 40% greater removal than the conventional coagulation—sedimentation process.  More than 95% turbidity, total solids, and total silica removal efficiencies were obtained.	Tsai et al. [92]
O&G SS from slaughterhouse wastewater	Pilot scale;  • 24 mg Al³+/L PACL  1.5 mg/L anionic polymer  • 100% influent pressurization at 300 kPa  • Lab scale (without coagulation);  • Pressure at 450 kPa  40% recycle ratio  • Lab scale (with coagulation);  • 24 mg Al³+/L PACL  • 1.5 mg/L anionic polymer  • Pressure at 450 kPa  • 40% recycle ratio	Using the pilot-scale full pressurization, the removal for SS and O&G was unsatisfactory at 28%–58% and 41%–57%, respectively.  Using the lab-scale DAF process (without coagulation), the removal was 54%–60% and 46%–74% for SS and O&G, respectively.  Using the lab-scale DAF process (with coagulation), the removal was 74% and 99% for SS and O&G, respectively.	de Nardi et al. [93]
BOD <sub>5</sub> and COD from meat industry wastewater	<ul> <li>Ferric chloride with 80 mg/L Fe<sup>3+</sup></li> <li>Pressure at 4.0 bars</li> <li>5 min saturation time</li> <li>20% recycle ratio</li> </ul>	60.5% and $78%$ removal for BOD <sub>5</sub> and COD from initial concentration of 1500 and 2900 mg/L, respectively.	de Sena et al. [94]
BOD <sub>5</sub> and COD from personnel care product wastewater	Coagulation/precipitation;  • 600, 800, and 700 mg/L, and optimum pH was 8.23%, 9.1%, and 6.9% for ferric chloride, ferric sulphate, and alum, respectively  Coagulation/DAF;  • 600, 800, and 700 mg/L, and optimum pH was 8.23%, 9.1%, and 6.9% for ferric chloride, ferric sulphate, and alum, respectively  • Pressure at 4.0 bars	COD removal; 75.8%, 77.5%, and 76.7% for ferric chloride, ferric sulphate, and alum, respectively. BOD <sub>5</sub> removal; 78%, 78.7%, and 74% for ferric chloride, ferric sulphate, and alum, respectively. COD removal; 71.5%, 67.7%, and 77.5% for ferric chloride, ferric sulphate, and alum, respectively. BOD removal was not significant between these three types of coagulants. The use of coagulation/DAF offers lower investment and running cost compared with coagulation/precipitation, around 27.3% and 23.7%, respectively.	El-Gohary et al. [95]

with previous studies [102,104], coagulation/sedimentation offers a good removal in landfill leachate treatment. However, in terms of chemical usage, the coagulation/sedimentation process needs double that required by the coagulation/DAF process. The proper determination of type and dosage of chemicals will not only improve the process but also influence the running cost as proved by El-Gohary et al. [95]. Based on the study carried out by El-Gohary et al. [95], the initial investment and the running cost for coagulation and sedimentation are higher by 27.3% and 23.7%, respectively, compared with coagulation/DAF. Besides, the land area required for coagulation/DAF is less by 30% compared with coagulation/sedimentation. As a result, coagulation/DAF is more economical compared with coagulation/sedimentation in treating wastewater [95].

## LIST OF NOMENCLATURE

A	Area (m²)
D	Drag force (kN)
μ	Dynamic viscosity (kg/m/s)
U	Terminal velocity (m/s)
A	Radius of sphere (m)
$\Sigma$	Density of sphere (kg/m³)
P	Density of liquid (kg/m³)
$p_{\mathrm{g}}$	Density of gas (kg/m³)
$\tilde{C}_{ m D}$	Drag coefficient
Re	Reynolds number
ν	Kinematic viscosity (m <sup>2</sup> /s)
R	Ratio of total removal of solid concentration after flotation to the inflow solid concentration = $1-C_0/C_i$
$C_0$	Effluent suspended solids
$C_{\rm i}$	Influent suspended solids
$V_{ m r}$	Rising velocity of a single particle/air bubble (m/s)
Q	Flow applied to the flotation unit (m <sup>3</sup> /s)
Ah	Horizontal area of the unit (m <sup>2</sup> )
V	Volume of bubble (m <sup>3</sup> )
$\Delta  ho$	Difference of density between liquid and gas (kg/m³)
S	Area of bubble (m <sup>2</sup> )
PB	Vapour pressure (Pa)
$x_{\rm B}$	Mol. fraction of the solute
$K_{\mathrm{B}}$	Constant
$C_{\rm S}$	Concentration of air in saturated liquid (mg/L)
P	Absolute pressure (Pa)
K	Henry's law constant (M/atm)
F	Efficiency factor (kPa/mg/L)
$a_{\rm p}$	Concentration of air precipitated on reducing the pressure to atmospheric (mg/L)
P	Saturator pressure in atmospheres
$C_{\rm r}$	Concentration of air released in the tank (mg/L)
$C_{\rm a}$	Concentration of air that remains in solution at atmospheric pressure (mg/L)
$R_{\rm r}$	Recycle ratio
K	Influent saturation factor

d

 $v_{\rm o}$ 

 $k_{\rm b}$ 

$\phi_b$	Bubble volume concentration
$p_{ m sat}$	Saturated density of air
$p_{ m w}$	Density of water (gm/cm <sup>3</sup> )
$P_{\mathrm{A}}$	Dissolved pressure (dyne/cm <sup>2</sup> )
$P_0$	Atmospheric pressure (dyne/cm²)
R	Gas constant (erg/K·mol)
T	Absolute temperature (K)
$M_{ m w}$	Molecular weight of water (g/g·mol)
$K_{ m H}$	Henry's law constant (dyne/cm <sup>2</sup> )
$V_{ m b}$	Volume of air occupied by a single spherical bubble (cm³)
h	Depth from the liquid surface to the bubble (cm)
σ	Surface tension (dyne/cm²)
$d_{\mathrm{a}}$	Volumetric mean diameter of bubble (cm)
G	Volumetric flow rate of air generated under decrease in pressure (cm <sup>3</sup> /s)
Q	Volumetric flow rate (cm³/s)
$\eta_1$	Collision efficiency
$\eta_2$	Attachment efficiency
$r_{\rm p}$	Particle radius (cm)
$R_{\rm b}$	Bubble radius (cm)
$p_{ m p}$	Particle density (gm/mL)
$G_{ m j}$	Body force acting on the particle
$V_{ m j}$	Particle velocity (cm/s)
$u_{\rm j}$	Velocity the fluid would have at the position of the particle if no particle were there (cm/s)
t	Time (s)
V	Component of particle velocity (cm/s)
$\mu_{\mathrm{f}}$	Fluid viscosity (kg/m/s)
<i>x</i> , <i>y</i>	Cartesian position coordinates (cm)
и	Component of velocity field due to bubble (cm/s)
v	Dimensionless component of particle velocity (cm/s)
K	Particle inertia parameter
G	Dimensionless settling velocity of particle (cm/s)
η	Single bubble collision efficiency
$u_0$	Water velocity (cm/s)
$c_0$	Suspended particle concentration upstream from the collector where the flow is
7	undisturbed by the presence of the grain
d	Grain diameter (cm)
$\eta_{\mathrm{D}},\eta_{\mathrm{I}},\eta_{\mathrm{G}}$	Theoretical values for single collector efficiency
Pe	Peclet number
$R_{\rm b}$	Bubble radius (cm)
$U_{\mathtt{b}}$	Bubble rising velocity (cm/s)
$D_{ m f}$	Particle diffusivity (cm²/s)
$d_{ m p}$	Diameter of suspended particle (cm)
1	D'

Diameter of collector or bubble (cm)

Approach velocity of fluid (cm/s)

Boltzmann's constant for bubble

 $\alpha_{nh}$  Attachment efficiency

 $N_{\rm b}$  Total number concentration of bubbles

 $A_{\rm b}$  Projected area of bubble (m<sup>2</sup>)  $N_{\rm p}$  Particle number concentration

D Effective depth of flotation chamber (m)  $V_T$  Vertical rise rate of suspended solids (m/s)

T Detention time (s)

 $A_s$  Surface area of flotation chamber (m<sup>2</sup>)

 $V_{\rm H}$  Horizontal velocity (m/s)

 $A_c$  Cross-sectional area of flotation chamber (m<sup>2</sup>)

W Width of the flotation chamber (m)

L Effective length of the flotation chamber (m)

## REFERENCES

- Rodrigues, R.T. and Rubio, J. (2007). DAF-dissolved air flotation: Potential applications in the mining and mineral processing industry. *International Journal of Mineral Processing*. Vol. 82, pp. 1–13.
- Merrill, C.W. and Pennington, J.W. (1962). The magnitude and significance of flotation in the mineral industries of the United States. In *Froth Flotation 50th Anniversary Volume* (Edited by Fuerstenau, D.W.), Chapter 4. The American Institute of Mining, Metallurgical, and Petroleum Engineers, Inc., New York.
- Travers, S.M. and Lovett, D.A. (1985). Pressure flotation of abattoir wastewaters using carbon dioxide. Water Research. Vol. 19, pp. 1479–1482.
- Krofta, M. and Wang, L.K. (1982). Potable water treatment by dissolved air flotation. *Journal American Water Works Association*. Vol. 74, pp. 305–310.
- Krofta, M., Wang, L.K., and Pollman, C.D. (1988). Treatment of seafood processing wastewater by dissolved air flotation, carbon adsorption and free chlorination. *Proceedings of the 43rd Purdue Industrial Waste Conference*, Purdue University, West Lafayette, IN, pp. 535–550.
- Wang, L.K. and Wang, M.H.S. (1989). Bubble dynamics and air dispersion mechanisms of air flotation process systems. Part A: Materials balances. *Proceedings of the 44th Purdue Industrial Waste Conference*, Purdue University, West Lafayette, IN, pp. 493–504.
- 7. Van Puffelen, J., Buijs, P.J., Nunn, P.A.N.M., and Hijnen, W.A.M. (1995). Dissolved air flotation in potable water treatment: The Dutch experience. *Water Science Technology*. Vol. 31, pp. 149–157.
- 8. Childs, A.R., Burnfield, I., and Rees, A.J. (1977). Operational experience with the 2300 m<sup>3</sup>/day pilot plant of the Essex Water Company. *Papers and Proceedings of the WRC Conference: Flotation for Water and Waste Treatment, Medmenham.*
- 9. Nickols, D., Moerschell, G.C., and Broder, M.V. (1995). The first DAF water treatment plant in the United States. *Water Science Technology*. Vol. 31, pp. 239–246.
- Edzwald, J.K. and Walsh, J.P. (1992). Dissolved air flotation: Laboratory and pilot plant investigation. AWWA Research Foundation and AWWA, Denver, CO.
- 11. Gregory, R. and Zabel, T.F. (1990). Sedimentation and flotation. In *Water Quality and Treatment: A Handbook of Community Water Supply* (Edited by Pontius, F.W.), 4th edition. McGraw Hill, New York, pp. 367–453.
- 12. Kitchener, J.A. (1984). The froth flotation process: Past and present and future-in brief. In *The Scientific Basis of Flotation* (Edited by Ives, K.J.). NATO ASI Series. Martinus Nijhoff Publishers, The Hague, the Netherlands, pp. 3–52.
- Lundgren, H. (1976). Theory and practice of dissolved air flotation. *Journal of Filtration and Separation*.
   Vol. 13, pp. 24–28.
- 14. Heinanen, J. (1988). Use of dissolved air flotation in potable water treatment in Finland. *Aqua Fennica*. Vol. 18, pp. 113–123.
- 15. Longhurst, S.J. and Graham, J.D. (1987). Dissolved air flotation for water treatment: A survey of operational units in Great Britain. *Public Health Engineering*. Vol. 14, pp. 71–76.
- 16. Zabel, T.F. (1978). Flotation. Twelfth International Water Supply Congress, Kyoto, Japan.

- 17. Packham, R.F. and Richards, W.N. (1975). Water clarification by flotation 3: Treatment of Thames water in a pilot-scale flotation plant. WRC Technical Report TR2, Medmenham, UK.
- 18. Zabel, T.F. (1985). The advantage of dissolved-air flotation for water treatment. *Journal American Water Works Association*. Vol. 77, pp. 42–46.
- 19. Gregory, R., Zabel, T.F., and Edzwald, J.K. (1999). Sedimentation and flotation. In *Water Quality and Treatment: A Handbook of Community Water Supplies* (Edited by Letterman, R.D.). McGraw-Hill, New York, pp. 7.1–7.87.
- 20. Ho, C.C. and Chan, C.Y. (1986). The application of lead dioxide-coated titanium anode in the electroflotation of palm oil mill effluent. *Water Research*. Vol. 20, pp. 1523–1529.
- 21. Zabel, T.F. and Melbourne, J.D. (1980). Flotation. Development in Water Treatment-1. Applied Science Publishers, London.
- 22. Barnes, D., Bliss, P.J., Gould, B.W., and Vallenrine, H.R. (1981). *Water and Wastewater Engineering Systems*, Chapter 8. Pitman Books Ltd., London.
- Zabel, T.F. and Hyde, R.A. (1977). Factors influencing dissolved air flotation as applied to water clarification. Papers and Proceedings of WRC Conference: Flotation for Water and Waste Treatment, Marlow.
- Zabel, T. (1984). Flotation in water treatment. In *The Scientific Basis of Flotation* (Edited by Ives, K.J.),
   NATO ASI Series. Martinus Nijhoff Publishers, The Hague, the Netherlands.
- 25. Al-Shamrani, A.A., James, A., and Xiao, H. (2002). Destabilisation of oil–water emulsions and separation by dissolved air flotation. *Water Research*. Vol. 36, pp. 1503–1512.
- 26. Edzwald, J.K. (2010). Dissolved air flotation and me. Water Research. Vol. 44, pp. 2077–2106.
- Haarhoff, J. and Steinbach, S. (1996). A model for the prediction of the air composition in pressure saturators. Water Research. Vol. 30, pp. 3074–3082.
- 28. Vesilind, P.A. (2003). Wastewater Treatment Plant Design. Water Environment Federation, New York.
- 29. HDR Engineering, Inc. (2001). Handbook of Public Water Systems. John Wiley & Sons, New York.
- Harper, J.F. (1972). The motion of bubbles and drops through liquids. In Advances in Applied Mechanics (Edited by Chia, S.Y.). Academic Press, New York, Vol. 12, pp. 59–129.
- 32. Li, W.H. and Lam, S.H. (1964). *Principles of Fluid Mechanics*. Addison-Wesley Publ. Co., Inc., Reading, MA.
- 33. Gaudin, A.M. (1939). Principles of Mineral Dressing, Chapter VIII. McGraw-Hill, London.
- 34. Batchelor, G.K. (1988). An Introduction to Fluid Dynamics. University Press, Cambridge, MA.
- 35. Shaw, D.J. (1991). *Introduction to Colloid and Surface Chemistry*, Chapter 1, 4th edition. Butterworth-Heinemann Ltd, Oxford.
- 36. Clift, R., Grace, J.R., and Weber, M.E. (1978). Bubbles, Drops, and Particles. Academic Press, New York.
- 37. Chorlton, F. (1967). Textbook of Fluid Dynamics, Chapter 8. D. Van Nostrand Co. Ltd., London.
- 38. Packham, R.F. and Richards, W.N. (1972). Water Clarification by Flotation 1: A Survey of the Literature. WRA Technical Paper TP87, Medmenham, UK.
- 39. Moore, W.D. (1965). The Velocity Rise of Distorted Gas Bubbles in a Liquid of Small Viscosity. *Journal of Fluid Mechanics* 23(04):749–766.
- Jameson, G.J. (1984). Experimental techniques in flotation. In *The Scientific Basis of Flotation* (Edited by Ives, K.J.), NATO ASI Series. Martinus Nijhoff Publisher, The Hague, the Netherlands, pp. 53–78.
- Shannon, W.T. and Buisson, D.H. (1980). Dissolved air flotation in hot water. Water Research. Vol. 14, pp. 759–765.
- 42. Fair, G.M., Geyer, J.C., and Okun, D.A. (1968). Water and Wastewater Treatment Engineering, Vol. 2, Chapter 26. John Wiley & Sons.
- 43. Vrablik, E.R. (1959). Fundamental principles of dissolved-air flotation of industrial wastes. *Proceedings of the 14th Industrial Waste Conference*, Purdue University, West Lafayette, IN, pp. 743–779.
- 44. Krofta, M. and Wang, L.K. (1989). Bubble dynamics and air dispersion mechanisms of air flotation process systems, Part B: Air dispersion. *Proceeding of the 44th Purdue Industrial Waste Conference*, Purdue University, West Lafayette, IN, pp. 505–511.
- 45. Fukushi, K., Tambo, N., and Matsui, Y. (1995). A kinetic model for dissolved air flotation in water and wastewater treatment. *Water Science Technology*. Vol. 31, pp. 37–47.
- 46. Edzwald, J.K., Malley, J.P, and Yu, C. (1990). A conceptual model for dissolved air flotation in water treatment. *Water Supply*. Vol. 9, pp. 141–150.
- Fukushi, K., Tambo, N., and Kiyotsuka, M. (1985). An experimental evaluation of kinetic process of dissolved air flotation. *Journal Japan Water Works Association*. Vol. 607, pp. 32–41.
- 48. Levich, V.G. (1962). Physicochemical Hydrodynamics. Prentice-Hall, Inc., Englewood Cliffs, NJ.

- Howe, R.H.L. (1958). A mathematical interpretation of flotation for solid-liquid separation. In *Biological Treatment of Sewage and Industrial Wastes*, Vol. 2 (Edited by McCabe, B.S. and Eckenfelder, W.W.). Reinhold Publishing Corp., New York, pp. 241–250.
- Karamanev, G.K. (1994). Rise of bubbles in quiescent liquids. *Journal American Institute Chemical Engineer*. Vol. 40, pp. 1418–1421.
- 51. Gerrard, W. (1980). Gas Solubilities Widespread Applications, Chapter 1. Pergamon Press, Oxford, UK.
- Lovett, D.A. and Travers, S.M. (1986). Dissolved air flotation for abattoir wastewater. Water Research. Vol. 20, pp. 421–426.
- 53. Backhurst, J.R., Harker, J.H., and Porter, J.E. (1974). *Problems in Mass Transfer*. Edward Arnold Ltd, London.
- 54. Atkins, P.W. (1994). Physical Chemistry, Chapter 7. Oxford University Press, Oxford, UK.
- 55. Takahashi, T., Miyahara, T., and Mochizuki, H. (1979). Fundamental study of bubble formation in dissolved air pressure flotation. *Journal Chemical Engineering Japan*. Vol. 12, pp. 275–280.
- 56. Ward, A.S. (1992). Dissolved air flotation for water and wastewater treatment. *Process Safety and Environmental Protection*. Vol. 70, pp. 214–218.
- Klassen, V.I. and Mokrousov, V.A. (1963). An Introduction to the Theory of Flotation. Butterworths, London.
- 58. Edwards, W.M. (1984). Mass transfer and gas absorption. In *Perry's Chemical Engineers' Handbook* (Edited by Green, D.W.), 6th Edition. McGraw-Hill, New York.
- 59. Eckenfelder, W.W. Jr., Rooney, T.F., Burger, T.B., and Gruspier, J.T. (1958). Studies on dissolved air flotation on biological sludges. In *Biological Treatment of Sewage and Industrial Wastes*, Vol. 2 (Edited by McCabe, B.S. and Eckenfelder, W.W.). Reinhold Publishing Corp., New York, pp. 241–250.
- 60. Bratby, J. and Marais, G.V.R. (1974). Dissolved air flotation. Filtration & Separation. Vol. 11, pp. 614-624.
- 61. Rykaart, E.M. and Haarhoff, J. (1995). Behaviour of air injection nozzles in dissolved air flotation. *Water Science Technology*. Vol. 31, pp. 25–35.
- 62. Gulas, V., Benefield, R.L., Lindsey, R., and Randall, C. (1980). Design considerations for dissolved air flotation. *Water & Wastewater Sewage Works*. Vol. 127, pp. 30–31, 42.
- 63. Ramirez, E.R. (1980). Comparative physicochemical study of industrial wastewater treatment by electrolytic, dispersed and dissolved air flotation technologies. *Proceedings of the 34th Industrial Waste Conference*, Purdue University, West Lafayette, IN, pp. 699–709.
- 64. Jones, A.D. and Hall, A.C. (1981). Removal of metal ions from aqueous solutions by dissolved air flotation. *Filtration & Separation*, September/October, pp. 386–390.
- Bratby, J. and Marais, G.V.R. (1975). Saturator performance in dissolved-air (pressure) flotation. Water Research. Vol. 9, pp. 929–936.
- 66. Cassell, E.A., Kaufman, K.M., and Matijevic, E. (1975). The effects of bubble size on microflotation. *Water Research*. Vol. 9, pp. 1017–1024.
- Collin, G.L. and Jameson, G.J. (1976). Experiment on the flotation of fine particles: The influence of particle size and charge. *Chemical Engineering Science*. Vol. 31, pp. 985–99.
- 68. Rovel, J.M. (1977). Experiences with dissolved air flotation for industrial effluent treatment. *Papers and Proceeding of the WRC Conference: Flotation for Water and Waste Treatment*, Bucks.
- 69. Reay, D. and Ratcliff, G.A. (1973). Removal of fine particles from water by dispersed air flotation. *The Canadian Journal of Chemical Engineering*. Vol. 51, pp. 178–185.
- Gochin, R.J. (1990). Flotation, In Solid-Liquid Separation (Edited by Svarovsky, L.), 3rd Edition. Butterworths, London, pp. 591–613.
- 71. Reay, D. and Ratcliff, G.A. (1975). Experimental testing of the hydrodynamic collision model of fine particle flotation. *The Canadian Journal of Chemical Engineering*. Vol. 53, pp. 481–486.
- 72. Flint, L.R. and Howarth, W.J. (1971). The collision efficiency of small particles with spherical air bubbles. *Chemical Engineering Science*. Vol. 26, pp. 1155–1168.
- 73. King, R.P. (1982). Flotation of fine particles. In *Principles of Flotation* (Edited by King, R.P.), South African Institute of Mining and Metallurgy, Johannesburg, South Africa, pp. 215–225.
- 74. Sutherland, K.L. (1948). Kinetics of the flotation process. *Journal Physical Colloid Chemistry*. Vol. 52, pp. 394–425.
- 75. Woodburn, E.T., King, R.P., and Colborn, R.P. (1971). The effect of particle size distribution on the performance of a phosphate flotation process. *Metallurgical and Material Transactions*. Vol. 2, pp. 3163–3174.
- 76. Yao, K.M., Habibian, M.T., and O'Melia, C.R. (1971). Water and waste water filtration: Concept and applications. *Environmental Science and Technology*. Vol. 5, pp. 1105–1112.

- 77. Malley, J.P. Jr. and Edzwald, J.K. (1991). Concepts for dissolved air flotation treatment of drinking waters. *Aqua*. Vol. 40, pp. 7–17.
- Friedlander, S.K. (1967). Particle diffusion in low speed flows. *Journal of Colloid Interface Science*. Vol. 23, pp. 157–164.
- O'Melia, C.R. (1985). Particles, pretreatment and performance in water filtration. *Journal of Environmental Engineering*. Vol. 111, pp. 874

  –890.
- 80. Katz, W.J. and Wullschleger, R. (1957). Studies of some variables which affect chemical flocculation when used with dissolved air flotation. *Proceedings of 12th Purdue Industrial Waste Conference*, Purdue University, West Lafayette, IN, pp. 466–479.
- 81. Eckenfelder, W.W. Jr. and O'Connor, D.J. (1961). *Biological Waste Treatment*, Chapter 5. Pergamon Press, London.
- 82. Noone, G. (1995). Personal Communication.
- 83. Bratby, J. and Marais, G.V.R. (1975). Dissolved air (pressure) flotation: An evaluation of inter-relationships between process variables and their optimisation for design. *Water S.A.* Vol. 1, pp. 57–69.
- 84. Edzwald, J.K. (1995). Principles and applications of dissolved air flotation. *Water Science and Technology*. Vol. 31, pp. 1–23.
- 85. Hyde, R.A. (1975). Water clarification by flotation-4, design and experimental studies on a dissolved air flotation plant treating 8.2 m<sup>3</sup>/h of River Thames Water. WRC Technical Report TR13, Medmenham, UK.
- 86. Haarhoff, J. and Vuuren, L.R.J. (1995). Design parameters for dissolved air flotation in South Africa. *Water Science and Technology*. Vol. 31, pp. 203–212.
- 87. Murshed, M.F. (2007). Removal of turbidity, suspended solid and aluminum using DAF pilot plant. MSc thesis, Universiti Sains Malaysia.
- 88. Adlan, M.N. (1998). A study of dissolved air flotation tank design variables and separation zone performance. PhD thesis, University of Newcastle Upon Tyne.
- 89. Ponasse, M., Dupre, V., Aurelle, Y., and Secq, A. (1998). Bubble formation by water release in nozzle II. Influence of various parameters on bubble size. *Water Research*. Vol. 32, pp. 2498–2506.
- 90. Al-Shamrani, A.A., James, A., and Xioh, H. (2002). Separation of oil from water by dissolved air flotation. *Colloids and Surfaces A: Physicochemical and Engineering Aspects*. Vol. 209, pp. 15–26.
- 91. Edzwald, J.K. (2006). Dissolved air flotation in drinking water treatment. Chapter 6 in *Interface Science in Drinking Water Treatment*, Vol 10, eds. G. Newcombe and D. Dixon. Elsevier, New York.
- 92. Tsai, J.C., Kumar, M., Chen, S.Y., and Lin, J.G. (2007). Nano-bubble flotation technology with coagulation process for the cost-effective treatment of chemical mechanical polishing wastewater. *Separation and Purification Technology*. Vol. 58, pp. 61–67.
- de Nardi, I.R., Fuzi, T.P., and Del Nery, V. (2008). Performance evaluation and operating strategies of dissolved-air flotation system treating poultry slaughterhouse wastewater. *Resources, Conservation and Recycling*. Vol. 52, pp. 533–544.
- 94. de Sena, R.F., Moreira, R.F.P.M., and Jose, H.J. (2008). Comparison of coagulants and coagulation aids for treatment of meat processing wastewater by column flotation. *Bioresource Technology*. Vol. 99, pp. 8221–8225.
- El-Gohary, F., Tawfik, A., and Mahmoud, U. (2010). Comparative study between chemical coagulation/ precipitation (C/P) versus coagulation/dissolved air flotation (C/DAF) for pre-treatment of personal care products (PCPs) wastewater. *Desalination*. Vol. 252, pp. 106–112.
- Zouboulis, A.I. and Avranas, A. (2000). Treatment of oil-in-water emulsions by coagulation and dissolved-air flotation. *Colloids and Surfaces A: Physicochemical and Engineering Aspects*. Vol. 172, pp. 153–161.
- 97. Bensadok, K., Belkacem, M., and Nezzal, G. (2007). Treatment of cutting oil/water emulsion by coupling coagulation and dissolved air flotation. *Desalination*. Vol. 206, pp. 440–448.
- 98. Hami, M.L., Al-Hash, M.A., and Al-Doori, M.M. (2007). Effect of activated carbon on BOD and COD removal in a dissolved air flotation unit treating refinery wastewater. *Desalination*. Vol. 216, pp. 116–122.
- Poha, P.E., Onga, W.Y.J., Laub, E.V., and Chonga, M.N. (2014). Investigation on micro-bubble flotation and coagulation for the treatment of anaerobically treated palm oil mill effluent (POME). *Journal of Environmental Chemical Engineering*. Vol. 2, pp. 1174–1181.
- Zouboulis, A.I., Jun, W., and Katsoyiannis, I.A. (2003). Removal of humic acids by flotation. *Colloids and Surfaces A: Physicochemical and Engineering Aspects*. Vol. 231, pp. 181–193.
- 101. Palaniandy, P., Adlan, M.N., Aziz, H.A., and Murshed, M.F. (2010). Application of dissolved air flotation (DAF) in semi-aerobic leachate treatment. *Chemical Engineering Journal*. Vol. 157, pp. 316–322.

- 102. Adlan, M.N., Palaniandy, P., and Aziz, H.A. (2011). Optimization of coagulation and dissolved air flotation (DAF) treatment of semi-aerobic landfill leachate using response surface methodology (RSM). *Desalination*. Vol. 277, pp. 74–82.
- Aziz, H.A., Alias, S., and Adlan, M. (2007). Colour removal from landfill leachate by coagulation and flocculation processes. *Bioresource Technology*. Vol. 98, pp. 218–220.
- 104. Lo, I.M.C. (1996). Characteristics and treatment of leachates from domestic landfills. *Environment International*. Vol. 22, pp. 433–442.
- 105. Ghafari, S., Aziz, H.A., and Bashir, M.J.K. (2010). The use of poly-aluminum chloride and alum for the treatment of partially stabilized leachate: A comparative study. *Desalination*. Vol. 257, pp. 110–116.
- 106. Bondelind, M., Sasic, S., Bergdahl, L. (2013). A model to estimate the size of aggregates formed in a dissolved air flotation. Applied Mathematical Modelling. Vol. 37, pp. 3036–3047.
- 107. Lakghomi, B., Lawryshyn, Y., and Hofmann, R. (2015). A model of particle removal in a dissolved air flotation tank: Importance of stratified flow and bubble size. *Water Research*. Vol. 68, pp. 262–272.
- 108. Zhanga, Q., Liu, S., Yang, C., Chen, F., Lu, S. (2014). Bioreactor consisting of pressurized aeration and dissolved air flotation for domestic wastewater treatment. Separation and Purification Technology. Vol. 138, pp. 186–190.